Investigation of Satellite Constellation Configuration for Earth Observation Using Sierra Nevada Dream Chaser® Spacecraft

Undergraduate Thesis

Presented in Partial Fulfillment of the Requirements for Graduation with Research Distinction
from the Department of Mechanical and Aerospace Engineering
The Ohio State University
Spring, 2018

Author

Andrew John Steen

Defense Committee

Dr. John M. Horack [Advisor]
Dr. Datta V. Gaitonde

Abstract

As the global climate crisis continues to drive extreme weather conditions, the need for increasingly robust systems to deliver unprecedented Earth Observation (EO) data will become a major economic concern for nations worldwide. The need exists for an international open platform for EO that can be utilized by small, less economically or technologically advanced nations for data acquisition as they attempt to deal with environmental disasters. The purpose of this project is therefore to develop an orbital strategy for the construction and utilization of an EO constellation of satellites, using as its platform the Sierra Nevada Corporation's Dream Chaser® spacecraft after its supply missions are completed at the International Space Station.

In this paper I summarize the current international access to highly temporally, spectrally, and spatially precise EO for close to real-time disaster response and the apparent lack thereof, I introduce the benefits of a collaborative and dynamic international platform under the initial context of a fleet of Dream Chaser orbital platforms, and detail the orbital mechanics theory and approach to enabling passively and actively responsive EO for the chosen relevant case study of the South East-Asian region. Initial results indicate that such a system could enable needed disaster response efforts from space in regions of the world with the least access to them but the highest need for them due to the onslaught of extreme weather patterns created by global climate change.

Acknowledgements

I would first like to thank my fantastic advisor, mentor, and friend, Dr. John Horack. John has for the last few years given me and my peers unprecedented access to the space community, allowing us to grow as engineers and young professionals beyond the traditional setting of the classroom. John and his efforts at Ohio State and beyond have given me motivation, encouragement, and confidence to seek out the incredible things space technologies and collaboration can do for our world, and to find my own role in their advancement.

As well, I would like to acknowledge the significant help that the Battelle Center for Science, Engineering, and Public Policy in the John Glenn College of Public Affairs has been in the progression of this research, as well as in the progression of myself as a student of the international community. The efforts of Dr. Elizabeth Newton have allowed me to conduct this research in Scotland with Stevenson Astrosat, Ltd. and present this research in person at the International Astronautical Congress in Australia this past year, all the while allowing me to follow a detailed course in practicing my presentation abilities and professional etiquette. I think any student would be fortunate to be part of such a great community.

I would also like to acknowledge and thank Dr. Robert Siston, and his efforts in seminars this past year. His class allowed me to practice my presentation abilities in depth, field and adapt to criticism, and create strategies for dealing with public speaking stress and anxiety.

And finally, I would like to extend my deepest gratitude to Mr. Steve Lee, CEO of Astrosat, for allowing me to conduct this research in his old kirk in Edinburgh, Scotland. I hope to return soon enough.

Table of Contents

Abstract ... **iii**
Acknowledgements ... **iv**
Table of Contents ... **v**
List of Figures ... **vi**
List of Tables ... **vii**
Chapter 1: Introduction ... **1**
1.1 Background ... 1
1.1.1 Global Climate Trends ... *1*
1.1.2 Economic & Climate Vulnerability of Emerging Economies ... *2*
1.1.3 International Access to Space-Borne Disaster Response ... *4*
1.2 Focus and Significance of Research ... 5
1.3 Overview of Thesis ... 6
Chapter 2: A Proposed Solution ... **7**
2.1 Solution Description ... 7
2.1.1 The Sierra Nevada Dream Chaser® ... *7*
2.1.2 Constellation Theory ... *8*
2.1.3 Reusability & Modularity ... *9*
2.2 Objectives of Solution ... 11
Chapter 3: Operational Strategy ... **12**
3.1 Orbital Mechanics Background Information ... 12
3.2 Deployment Strategy ... 13
3.2.1 Conventional Deployment ... *13*
3.2.2 ISS CRS-2 Deployment ... *14*
3.3 Constellation Configuration Theory ... 16
3.3.1 Nodal Precession ... *17*
Chapter 4: Computational Methods ... **19**
4.1 Computational Modelling Theory ... 19
4.2 Systems Tool Kit® Scenario Set-up ... 22
4.3 Data Output ... 25
Chapter 5: Results and Analysis ... **26**
Chapter 6: Conclusion ... **30**
Appendix A ... **32**
Appendix B ... **40**
References ... **41**

List of Figures

Figure 1: Verisk Maplecroft Climate Change Vulnerability Index Map (2017) 2
Figure 2: SNC Dream Chaser Cargo Variant 7
Figure 3: Dream Chaser Long Duration Earth Observation Variant 10
Figure 4: Geometry of Elliptical Orbits 12
Figure 5: Orbital Plane Parameters 13
Figure 6: ISS Nodal Precession after 100 Days 19
Figure 7: STK Area Definition for EO Ground Coverage Analysis 23
Figure 8: Example of Dream Chaser Satellite Object Initialization 24
Figure 9: Sensor Object Definition for Each Dream Chaser 24
Figure 10: Ground Coverage Definition Assets 25
Figure 11: Example Graphical Output in STK for Figure of Merit 25
Figure 12: 3(51.64°); 2(30°):/5/5/1 Average Revisit Times 27
Figure 13: 3(51.64°); 2(30°):/5/5/1 Total Coverage Times 28
Figure A1: 51.64°:/5/5/1 Average Revisit Times 32
Figure A2: 51.64°:/5/5/1 Total Coverage Times 32
Figure A3: 51.64°:/5/5/1 Revisit Time Per Latitude 33
Figure A4: 51.64°:/5/5/1 Coverage Time Per Latitude 33
Figure A5: 3(51.64°); 2(30°):/5/5/1 Average Revisit Times 34
Figure A6: 3(51.64°); 2(30°):/5/5/1 Total Coverage Times 34
Figure A7: 3(51.64°); 2(30°):/5/5/1 Revisit Time Per Latitude 35
Figure A8: 3(51.64°); 2(30°):/5/5/1 Coverage Time Per Latitude 35
Figure A9: (15°, 17.5°, 20°, 22.5°, 25°): 5/5/1 Average Revisit Times 36
Figure A10: (15°, 17.5°, 20°, 22.5°, 25°): 5/5/1 Total Coverage Times 36
Figure A11: (15°, 17.5°, 20°, 22.5°, 25°): 5/5/1 Revisit Time Per Latitude 37
Figure A12: (15°, 17.5°, 20°, 22.5°, 25°): 5/5/1 Coverage Time Per Latitude 37
Figure A13: 15°:/5/5/1 Average Revisit Times 38
Figure A14: 15°:/5/5/1 Total Coverage Times 38
Figure A15: 15°:/5/5/1 Revisit Time Per Latitude 39
Figure A16: 15°:/5/5/1 Coverage Time Per Latitude 39
Figure B1: Example of Typical Hohmann Transfer Strategy 40

List of Tables

Table 1: Internationally Accessible Satellite Data Examples....4
Table 2: ISS Zarya (25544) Orbital Elements....14
Table 3: Hohmann Transfer ΔV Results for DC Leaving ISS Orbit....15
Table 4: Separation of RAAN of Each DC from ISS....18
Table 5: Tested Walker Delta Constellation Configurations....14

Chapter 1 – Introduction

1.1 Background

1.1.1 Global Climate Trends

The past few decades have seen more than their fair share of disastrous weather events, scales of which few events prior have any chance to match in severity, loss of life, and economic impact. And, while the general populous and those holding public office still debate voraciously the attribution of increasingly intense and frequent extreme weather patterns to human impact, the trend of increasingly extreme weather patterns persists, and negatively impacts billions globally. Regardless of the causality, numerous short and long-term climate extrapolation models predict a continuing increase in intensity and frequency of certain extreme weather patterns such as hurricanes, flash-floods due to storm surges, and dangerous heat waves.

Global oceanic heat content has increased steadily since measurements began in 1958 by NOAA and shows a close correlation with the global rise in atmospheric carbon dioxide concentration (Cheng et al., 2017). This increase in global water heat content has constituted a rise in global sea temperatures. Researchers have run various tropical storm models to predict the effect of this increase on global storm intensity and frequency. Although there is still some disagreement on specific expected trends, most note that while extreme tropical storms should decrease in frequency in certain regions, global tropical storm intensity is set to increase heavily in an even warmer mid to late 21st century climate (Knutson et al., 2010). This increase in intensity in tropical regions will continue to batter populations in tropical regions, who are consistently those least capable economically of dealing with disastrous weather events.

1.1.2 Economic & Climate Vulnerability of Emerging Economies

There are numerous global risk-management organizations that publish annually updated national and regional indices for vulnerability to a multitude of international concerns, such as the increase in extreme weather patterns and other issues often attributed to global climate change. Figure 1 below contains the global climate change vulnerability index map published by Verisk Maplecroft for 2017.

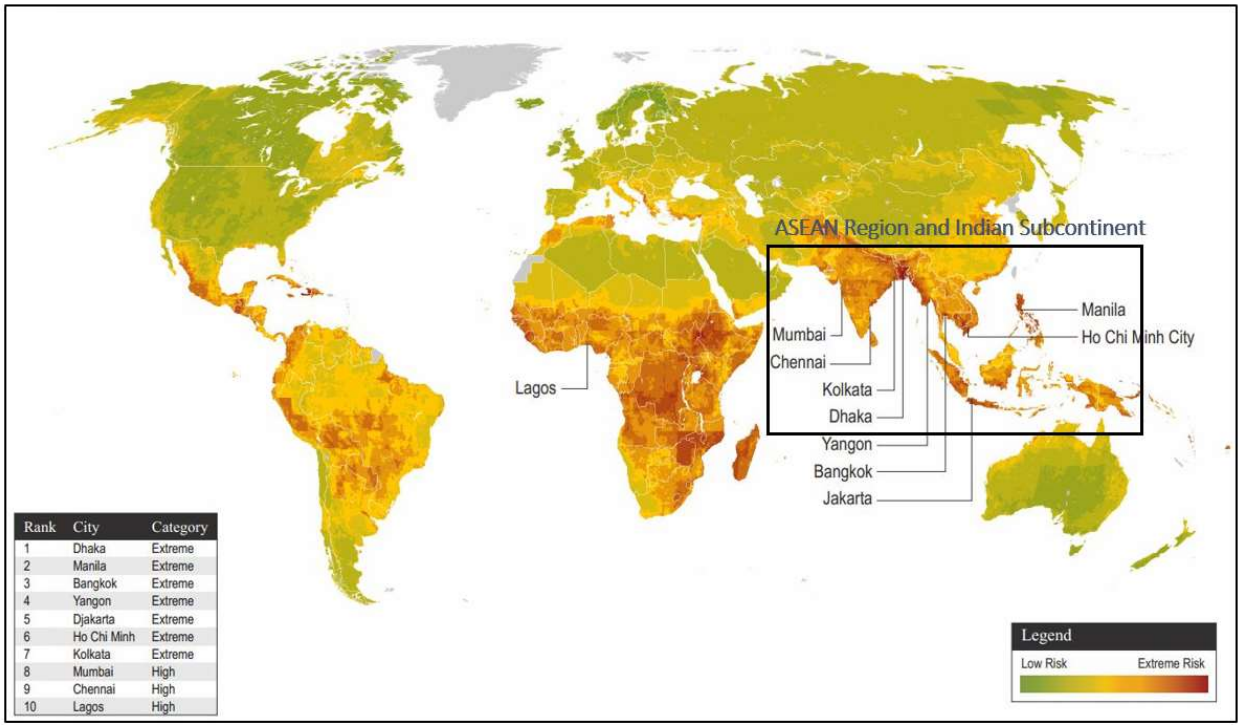

Rank	City	Category
1	Dhaka	Extreme
2	Manila	Extreme
3	Bangkok	Extreme
4	Yangon	Extreme
5	Djakarta	Extreme
6	Ho Chi Minh	Extreme
7	Kolkata	Extreme
8	Mumbai	High
9	Chennai	High
10	Lagos	High

Figure 1 – Verisk Maplecroft Climate Change Vulnerability Index Map (2017)

This map, while high-leveled and lacking in specific information such as population density dynamics and further environmental concerns, paints a qualitative picture of the concentration of vulnerability on a global scale. It is clear that there are areas that will be more highly impacted by climate change and extreme weather conditions. The dark red areas along the equator demonstrate concern for the larger population densities that the countries along those latitudes tend to contain.

Therefore, it is perhaps relevant to fix a socioeconomic analysis of a smaller region on the

globe for the purpose of this project. The case-study was chosen to be defined as the ASEAN (Association of Southeast Asian Nations) Region and the Indian Subcontinent, constrained approximately by latitudes of -10° to 30° and longitudes of 70° to 145°. Some major population centers in this region can be found in India, Bangladesh, Thailand, Malaysia, Indonesia, and Vietnam – contributing to a total case-study population of about 1.963 billion, without counting southern China (World Bank Open Data 2018). This number amounts to approximately 26% of the global population, within an area only about 1.1% of Earth's total land area ("Selected basic ASEAN indicators", 2014). Mean population density is therefore around 385 people per square kilometer, or about three times the population density of continental Europe. However, local population densities of the various metropolitan areas can reach as high as 41,515 persons per square kilometer in Manila or 28,508 persons per square kilometer in Mumbai, which contain approximately 1.78 and 12.5 million people, respectively ("List of cities by population density", 2018). This region is therefore a relevant case-study in this research, due to high coastal population densities and magnitudes present in areas most overall vulnerable to global climate change.

Dozens of recent disasters in the ASEAN region and Indian subcontinent have proven the drastically lopsided vulnerability to climate disasters both geographically and geo-economically. 2017 saw massive torrential downpours around India, Nepal, and Bangladesh, initiating floods that affected or displaced nearly 41 million people in the region ("South Asia: Flooding – Humanitarian Snapshot", 2017). This increase in precipitation in the summer monsoon months can possibly validate the study done by Cruz et al., which noted increasing temperature trends in India, Nepal, and Bangladesh changes in precipitation resulting in rain anomalies above decades long averages (Cruz et al, 2007). A few months later, Vietnam saw one of its worst typhoons in decades, Typhoon Damrey, which caused damages costing just shy of US$1.0 billion, nearly 0.5% of Vietnam's

yearly gross domestic product ("Viet Nam: Typhoon Damrey …", 2017). In such tropical regions response can be slow, as international NGOs and local relief efforts identify how to help, who and what to send, and what regions need the most immediate help. And as such, needs remain for housing, food, and water help spread across 15 provinces in Vietnam's central regions. As disasters like this and their less than perfect relief efforts last months and months after the extreme weather passes, increasingly harsh seasons will compound upon each other and create international situations cascading out of reach of reasonable mitigation and response.

1.1.3 International Access to Space-Borne Disaster Response

One way to supplement the relief and disaster mitigation efforts on the ground is by remotely-sensed data provided by space-borne platforms in orbit around the Earth. Satellites have long been platforms for complex data sources, sensing either passively via solar radiation reflected by the Earth or actively such as with lasers or synthetic aperture radar (SAR). Table 1 below contains some of the free internationally available satellite platforms, their data types, resolutions, and orbital configurations.

Table 1 – Internationally Accessible Satellite Data Examples

Platform Name	Organization	Purpose	Data Type [Sensor]	Spatial Res.	Spectral Range	Temporal Res.	Orbit Type
Landsat 7	USGS	Earth Imaging	Optical [ETM+]	30 m (60 thermal, 15 m pan)	0.45 - 12.5 µm	~16 days	Sun-synch (i=98.2°, h=702km)
Landsat 8			Opitcal [OLI]	30 m (15 m pan)	0.435 - 1.384 µm		
			Thermal [TIRS]	100 m (resampled to 30 m)	10.60-12.51 µm		
Aqua (EOS PM-1)	NASA	Earth Science	Optical [MODIS]	250 m - 1 km	0.4-14.5 µm	~1-2 days	Sun-synch (i=98.2°, h=702km)
			Visible/IR [AIRS]	2.3 km (visible), 13.5 km (IR)	0.41-0.94 µm (multispectral), 3.7-15.4 µm (hyperspectral)		
Terra (EOS AM-1)			Optical [MODIS]	250 m - 1 km	0.4-14.5 µm		
Sentinel 2A	ESA	Land and Sea Monitoring	Optical/IR [MSI]	10m (optical, pan), 20m (NIR, IR) , 60m (coastal, SWIR)	443.2-2185.7 nm	~5 days	Sun-synch (i=98.5623°, h=788km)
Sentinel 2B							
Sentinel 1	ESA	Land and Sea Monitoring	Synthetic Aperture Radar [C-SAR]	5m - 100m (4 different modes)	~5.5 cm (one frequency)	~12 days	Sun-synch (i=98.2°, h=693km)

These satellite platforms vary heavily from one to the next in their radiometric, spatial, and temporal resolutions, and are therefore useful for the large variety of purposes for which remote sensing has identified itself useful. Most satellites, however, once put into their respectively orbit patterns are rarely able to be changed in their trajectories, and so their uses are often predetermined far before launch. Although there are still some platforms that perform excellently for many uses – as they maintain necessary tradeoffs between the three types of aforementioned resolutions – in order to achieve near global coverage, they are often put into slightly retrograde polar orbits, which unfortunately limit temporal resolution globally. Therefore, remote sensing with this type of approach does not truly allow for timely active disaster response and monitoring, as disasters do not time their touchdowns based on the acquisition windows of orbiting satellites.

For disaster mitigation, satellites are still an excellent method by which vulnerability and risk management maps may be created, extrapolation models based on current and past flood, fire, and storm events can be facilitated, and climate research on a global scale can be conducted (Walter, 1990). But there are no platforms that exist specifically for real time disaster response and relief efforts. There are multiple reasons behind this lack of infrastructure, the largest being the cost of such a platform using conventional methods of launch and deployment.

1.2 Focus and Significance of Research

With the aforementioned limitations in the space technology landscape in mind, the purpose of this research is to propose a solution that can be implemented rapidly, economically, repeatably, and modularly for the specific purpose of disaster response and relief from space. The solution should take into consideration the diversity of disaster types, the need for highly temporally resolute data during specific times of the calendar year at which extreme weather is

most prevalent, and the reusability as a way to introduce better technologies into the system as well as save cost of launch and manufacturing.

The proposed solution will seek specifically to satisfy the apparent needs of the target case-study, while keeping in mind the broader significance that such a system if implemented could represent globally.

1.3 Overview of Thesis

In this paper, I will detail the proposed solution of the constellation of Sierra Nevada Dream Chasers. I will offer orbital mechanical theory behind the proposal, as well as some initial calculations proving its technical viability. The different configurations that will be tested will be discussed in detail, and explanations for motivation behind each will be offered.

Computational/experimental methods will be discussed in depth, and results pulled from the computational software will be analyzed for the metrics discussed in the following sections. These metrics will be analyzed, and qualitative and quantitative insights will be pulled from them in an effort to validate or invalidate each of the offered configuration.

And finally, a conclusion will be made on the viability and feasibility of the proposed concept in the broader context of international disaster response efforts.

Chapter 2 – A Proposed Solution

2.1 Solution Description

2.1.1 The Sierra Nevada Dream Chaser®

The solution proposed in this paper involves the retrofitting and utilization of the Dream Chaser® lifting body currently in production and later stages of testing by Sierra Nevada Corporation (SNC) of the United States. Dream Chase is a horizontal-landing capable space-plane, created initially for manned missions to LEO and beyond, later repurposed for cargo needs for NASA and the International Space Station under the guise of the CRS-2 (Cargo Resupply) missions. This spacecraft would not only be modular via industry standard connections and fittings but would be totally reusable via its horizontal-landing capabilities at most commercial airports around the globe. The Dream Chaser could therefore become the end-all beat-all EO platform via regular landing, refitting with latest sensors, and redeployment via a number of possible methods. A number of these spaceplanes, if placed in certain constellation configurations, would offer a unique opportunity to satisfy the gaps in disaster response for the case-study area and the international community. Figure 2 below displays the SNC Dream Chaser Cargo Variant.

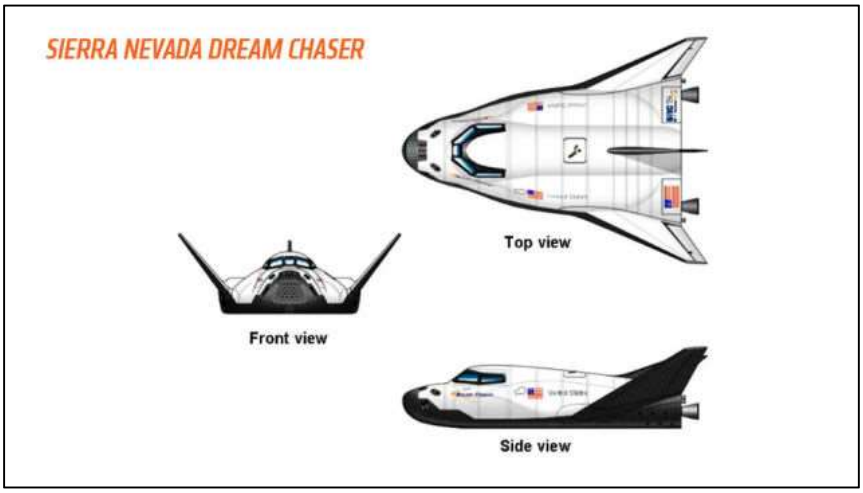

Figure 2 – SNC Dream Chaser Cargo Variant
[Courtesy: Sierra Nevada Corporation]

Dream Chaser is an effective vehicle choice for many reasons. Apart from its nearly-developed hardware status, each vehicle has its own ΔV capability for orbital readjustment and landing. Significant payload capacity is available, with complementary data and power provision (Olson, 2014). Each vehicle is a lifting body design, and therefore can be landed at most commercial airports around the globe, making orbital planning for re-entry simple compared to landing at only one or two potential sites. Finally, the multiple flight opportunities either with conventional launch in most launch vehicles with 5-meter fairings or via a unique in-orbit deployment following the CRS-2 missions mean that there are possibilities for using these space-planes in orbit as a distributed constellation for disaster response EO.

The collaborative deployment of such a constellation would present an opportunity for many emerging economies – those often the most disproportionately unable to combat their climate change and weather disaster threats – to pool their resources into a shared and robust option for EO, responding to adverse events which could have severe economic and humanitarian consequences which do not stop at national boundaries.

2.1.2 Constellation Theory

As mentioned, the Dream Chaser's could be deployed via a number of methods. The most common deployment method is of course launch via a launch vehicle on the surface at one of dozens of launch sites around the globe. For the Dream Chaser being produced by an American government contractor, any launch site would almost certainly have to be in the United States, where there is a wide range of capabilities for the type of mass that this vehicle would have for this type of mission. The only main constraint other than mass on the launch of this vehicle would be the fairing of the launch vehicle, which would have to be at least 5-meters such as on an Atlas

V or Falcon 9. This method will therefore not be under much scrutiny for the purpose of this paper but will only be considered as an alternative method of deployment to the novel condition to be introduced in the rest of this section.

The novel approach to deployment of the Dream Chaser by orbital repositioning following the cessation of the CRS-2 mission at the ISS by NASA will constitute most of the theory and investigation in this paper. This method would save a significant amount of money often needed to launch the platform initially, as it would "piggy back" off of the CRS-2 mission, allowing NASA to pay for the launch costs in order to receive its cargo from the Dream Chaser. Under the conditions of the CRS-2 mission, the Dream Chaser would deliver its cargo to the ISS, receive cargo that it would then jettison to be burned up in the atmosphere via an attach "trash" cargo module, and then undergo a de-orbiting maneuver, land, and then be refitted and relaunched for the same mission over a number of months (Olson, 2014). If instead, the Dream Chaser were to be propagated into a constellation of other Dream Chasers by a combination of impulse orbital maneuvers and natural anomalies, conditions could be created in which certain target areas on the globe such as the chosen case-study area could see potentially highly temporal data acquisition for the purpose of disaster response and monitoring. The propagation of these spacecraft into a few potential configurations will therefore be investigated in this paper, and parameters such as temporal resolution and total coverage time will be analyzed.

2.1.3 Reusability & Modularity

SNC has developed multiple possible commercial uses for the Dream Chaser beyond that of a cargo carrier for NASA. Its idea to use the vehicle as a sort of "space utility vehicle (SUV)" highlights the purposeful modularity that the system was made to contain from the beginning. For

example, an “observing from space” configuration of the Dream Chaser, the variation this project would hope to utilize, would allow for the spacecraft to be fitted with solar arrays, non-propulsive attitude control systems (to save ΔV), and a commercial relevant payload interface for a duration of up to one year (Olson, 2014). Figure 3 below contains an image of what an EO variant of the Dream Chaser could look like.

Figure 3 – Dream Chaser® Long Duration Earth Observation Variant

This purposeful modularity included in the very design of the Dream Chaser by SNC means that commercial options such as the one proposed in this project are likely well within the bounds of future possibilities for this product, both technically and operationally. The commercial payload interface available on the Dream Chaser would allow the latest, most relevant sensors to be equipped, allowing the system to maximize conditions such as technological advances in hyperspectral imaging with high spatial resolution, as well as novel approaches to complex remote sensing such as synthetic-aperture radar (SAR).

2.2 Objectives of Solution

The Dream Chaser constellation configurations will be chosen to attempt to minimize the average revisit times and maximize the average total coverage times per each month for a chosen time frame for the case-study area. These will be simulated and output within the AGI Systems Tool Kit (STK) workspace, analyzed over chosen months over the course of a whole year in order to see the properties of the progression of the constellation orbital parameters. The chosen configurations will also seek to take advantage of nodal regression, a natural process created by the oblation of the Earth's geopotential model, to be discussed further in this paper.

The configurations will also be considered for their economic viability by limiting ΔV budgets and thereby limiting propulsive mass needed, as well as limiting number of launches not covered by NASA by deploying within the context of the CRS-2 missions.

Chapter 3 – Operational Strategy

3.1 Orbital Mechanics Background Information

In order to discuss the orbital strategy of such a system, it is useful to outline the classical Keplerian elements that describe the orbit trajectories. Classical Keplerian orbital mechanics rely on the model of two point-mass objects exerting constant gravitational force on each other, with one mass (the Earth) significantly larger than the other (the spacecraft) that the small mass can be said to have negligible effect on the larger. Objects orbiting around each other have trajectories which can be described mathematically as conic sections – ellipses being the case for objects in captive orbits around the Earth.

The precise shape of a satellite's motion around the Earth is therefore principally described by its eccentricity (e) and the semimajor axis (a) of an ellipse. Figure 4 below outlines the basic structure of an elliptical orbit with the Earth at one focus.

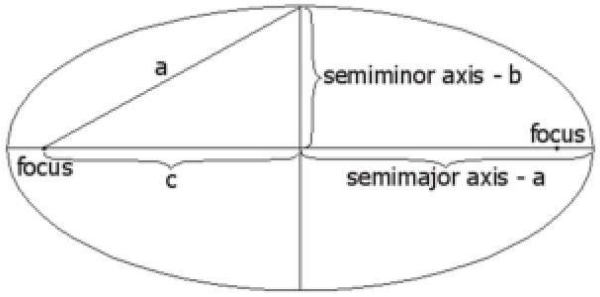

Figure 4 – Geometry of Elliptical Orbits

The eccentricity of the orbit is described in terms of the semi-major and semi-minor axes through the equation

$$e = \frac{c}{a} = \sqrt{1 - \left(\frac{b}{a}\right)^2} \tag{1}$$

Figure 5 on the following page outlines the further parameters that described the motion of the satellite as it travels around the ellipse, in relation to the Earth inertial frame.

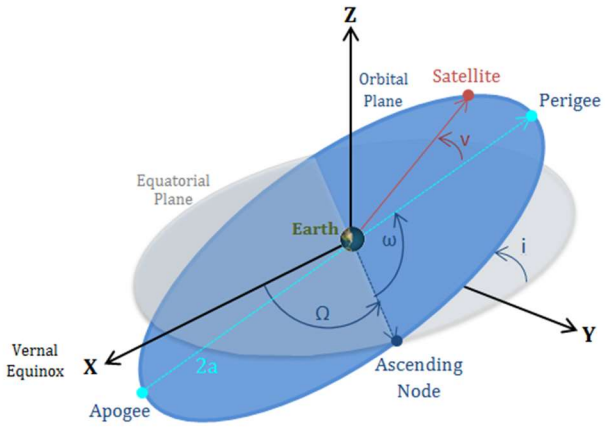

Figure 5 – Orbital Plane Parameters

Shown above are the additional three parameters needed to describe the orientation of the orbit. Therefore, a total of six parameters – semi-major axis (a), eccentricity (e), inclination (i), right ascension of the ascending node (RAAN or Ω), argument of perigee (ω), and true anomaly (ν) – are sufficient to describe fully the basic motion of satellite around the Earth and are used in calculations and simulations for this paper.

3.2 Deployment Strategy

3.2.1 Conventional Deployment

Conventional deployment of the Dream Chasers, as opposed to the novel method of deploying from the ISS following the cessation of the CRS-2 missions, would involve vertical launch from a typical launch vehicle on Earth. If launched, for example, from a 5-meter fairing capable launch vehicle such as the SpaceX Falcon 9, this would cost around US$57 million per Dream Chaser in order to add each to its spot in the constellation configuration (Chaikin, 2012). While this would be extremely more expensive than the ISS deployment, it would allow the Dream Chaser to be forced into any orbital configuration needed without need for huge orbital maneuvers in orbit, by allowing the second stage of the rocket to impart the ΔV needed to enter whatever inclination or RAAN necessary.

3.2.2 CRS-2 ISS Deployment

In order for each DC to separate its respective trajectory from the ISS and join/initiate an EO constellation, it would have to undergo a series of orbital maneuvers. The following Table 2 contains representative orbital elements for the ISS obtained in July 2017 from spaceflight.nasa.gov.

Table 2 – ISS Zarya (25544) Orbital Elements
Epoch (UTC): **05 Jul 2017 06:28:58**

a:	6782.83 [km]
e:	0.0005096
i:	51.6427°
Ω:	308.1913°
ω:	2.4396°
ν:	200.7582°

For the sake of computational precision and continuity, the classical orbital elements and epoch listed in Table 2 will be the datum used for all calculations and simulations in this paper. The altitude of apogee and perigee are found to be 408 and 401 kilometers, respectively. Each DC would then have to undergo an orbital maneuver to a higher altitude in order to take advantage of better ΔV budgeting for possible plane change maneuvers and different relative nodal precession rates to the ISS, which will be discussed further in the following subsection.

A Hohmann Transfer insertion orbit would be the optimum type of maneuver for this type of in place altitude change, assuming near-impulsive velocity change by the Dream Chasers. This assumption can vary in reliability based on the final specific impulse (Isp) of the Dream Chasers' main propulsion motors, which have yet to be published yet. However, considering that each will utilize hybrid propulsion, it can be assumed that the Isp will be relatively high (Sutton, 2010). The altitude to which each DC would initially ascend would be determined by mission goals, operational time scales, fleet size, and available ΔV budgeting with the intention of saving enough

capability to descend to an altitude at which each DC would enter the atmosphere and land.

A Hohmann Transfer consists of two burns, one to enter an eccentric orbit, and one to circularize at apogee of that eccentric orbit, creating a circular orbit with a larger or smaller altitude than the initial orbit. For the scope of this project, we will assume that all of the spacecraft will exist in purely circular orbits after deployment from the lowly-eccentric ISS orbit. The following set of formulas describe the Hohmann Transfer strategy.

$$a_{trans} = \frac{R+R'}{2} \qquad V_{trans,1}^2 = \mu\left(\frac{2}{R} - \frac{1}{a_{trans}}\right) \tag{2,3}$$

$$\Delta V = V_{trans,1} - \sqrt{\frac{\mu}{R}} \qquad V_{trans,2}^2 = \mu\left(\frac{2}{R'} - \frac{1}{a_{trans}}\right) \tag{4,5}$$

$$\Delta V' = \sqrt{\frac{\mu}{R'}} - V_{trans,2} \qquad \Delta V_{total} = |\Delta V + \Delta V'| \tag{6,7}$$

Where

μ = standard gravitational parameter of the Earth (**3.986e14** [m^3 s^{-2}])

$R', \Delta V'$ = radius and required ΔV at apogee of eccentric transfer orbit

Figure B1 in Appendix B displays an image of a typical Hohmann Transfer orbit for reference. Table 3 below contains the ΔV results for sending each Dream Chaser to various higher altitudes from the ISS datum listed previously. It should be noted that the spacecraft would need to do its initial burn at the point in its orbit when it is at maximum velocity – at ISS perigee of 401 kilometers – for the following results to be valid.

Table 3 – Hohmann Transfer ΔV Results for DC Leaving ISS Orbit at **05 Jul 2017 06:28:58 UTC**

ΔAlt. [km]	Final Alt. [km]	Semi-Major Axis [km]	ΔV [m/s]
100	501	6886.28	55.859
150	551	6936.28	83.319
200	601	6986.28	110.491
250	651	7036.28	137.371
300	701	7086.28	163.963
350	751	7136.28	190.273
400	801	7186.28	216.303

The total amount of ΔV expected to be available on each Dream Chaser has yet to be released to the public, although these numbers are a conservative number that should be possible by such a robust system.

3.3 Constellation Configuration Strategy

The constellations will need an efficient, practical method by which the ground tracks of each subsequent Dream Chaser can be separated from that of the ISS. For the configurations utilizing the deployment from the ISS rather than through conventional launch and deployment, a way in which to alter the orbital plane must be determined for both changes in inclination and right ascension of the ascending node (RAAN). Changes in argument of perigee will not be needed as the orbits will be assumed to be circular. A deliberate change of inclination and/or RAAN would involve an orbital plane change maneuver. For an orbit with an effectively circular shape (e ≈ 0), the ΔV can be calculated as follows

$$\Delta V_{i \text{ or } \Omega} = 2V sin\left(\frac{\Delta i \text{ or } \Delta\Omega}{2}\right) \tag{8}$$

It is clear by equation 8 that an orbital plane change maneuver is a highly inefficient maneuver to spend ΔV on – as, for example, a change in 45° of inclination or RAAN at 701 kilometers would cost well over 5,700 [m/s], which when considering the tyranny of the Tsiolkovsky Rocket equation would require tens of thousands of kilograms of propellant mass. Therefore, it should be assumed that any deliberate orbital plane change maneuver should be limited to small changes, such as for station keeping purposes. So, in order to build the constellation effectively by separating ground tracks, the Dream Chasers would have to take advantage of the natural process of nodal precession.

3.3.1 Nodal Precession

Nodal precession is the regression of the line of nodes in relation to the inertial frame of Earth due to the oblateness of the Earth at its equator contributing to a non-spherical geopotential model. The angular location of the line of nodes in the plane of the orbit is denoted by the right ascension of the ascending node, or RAAN. The following formula described the rotation of RAAN over time due to the 2nd zonal harmonic coefficient J_2 (Griffin, 2004)

$$\frac{d\Omega}{dt} = -\left(\frac{3}{2}\right) n J_2 \left(\frac{R_e}{a}\right)^2 \frac{\cos i}{(1-e^2)^2} \tag{9}$$

Where

J_2 = 2nd zonal harmonic coefficient of non-spherical geopotential model (**1.0826e-3**)

R_e = Earth mean volumetric radius (**6,371** [km])

On Earth, J_2 is dominant by all other coefficients of the Legendre Polynomials used to describe a planet's geopotential model, therefore it is sufficient to describe the perturbation of the line of nodes by the first order formula shown in equation 9. This same perturbation also perturbs the argument of perigee of an elliptical orbit, however this is arbitrary for circular orbits. Similarly, the effects of non-spherical oblation on semi-major axis, eccentricity, and inclination can be shown to be arbitrary or at least periodical with negligible amplitudes (Griffin, 2004).

This natural change in time of the RAAN essentially means that a relative separation of ground track from the ISS for each Dream Chaser to be deployed in that manner can be achieved without the need for ΔV expenditure beyond changing the altitude of the orbit or other potential reconfiguration maneuvers. Once each spaceplane reaches its target altitude, it can then simply "wait" as nodal precession rotates its orbital plane and ground track from the ISS, enabling the deployment of a multi-plane constellation. Table 4 on the following page summarizes the *relative* RAAN change of each Dream Chaser from the ISS at altitude, using equation 9 and the Keplerian

elements defined in Tables 2 and 3.

Table 4 – Separation of RAAN of Each DC from ISS due to Nodal Precession

Days Passed	ΔΩ [deg]
(501 [km])	
90 days	20.01
180 days	40.01
(551 [km])	
90 days	30.72
180 days	61.44
(601 [km])	
90 days	41.09
180 days	82.19
(651 [km])	
90 days	51.14
180 days	102.27
(701 [km])	
90 days	60.86
180 days	121.72
(751 [km])	
90 days	70.28
180 days	140.57
(801 [km])	
90 days	79.41
180 days	158.83

Clearly shown by Table 4, RAAN separation due to nodal precession would be an effective and practical method for ground track separation, operating within reasonable timeframes, the higher altitudes having more rapid RAAN separation. The mission altitudes would therefore be chosen after careful consideration of the mission constraints, namely on-board ΔV, expected potential viewing areas, and mission timescales. These constraints will determine the rate at which each Dream Chaser is able to separate from one another and from the ISS, and which will be the primary driver of ground coverage capabilities of the constellation.

Figure 6 on the following page is a visual example of nodal precession, simulated in STK for the ISS propagated with a first order J_2 Propagator for 100 days. The RAAN and therefore the ground track of the future position of the ISS has changed by about 34 degrees, which is predicted by equation 9. Note that the two represented orbital trajectories are not concurrent in time, rather that the yellow ISSPlus100Days is the trajectory of the ISS after it has propagated without force

input than J_2 perturbation for 100 days, shown graphically next to the ISS at its datum epoch of 05 Jul 2017 06:28:58.000 UTC.

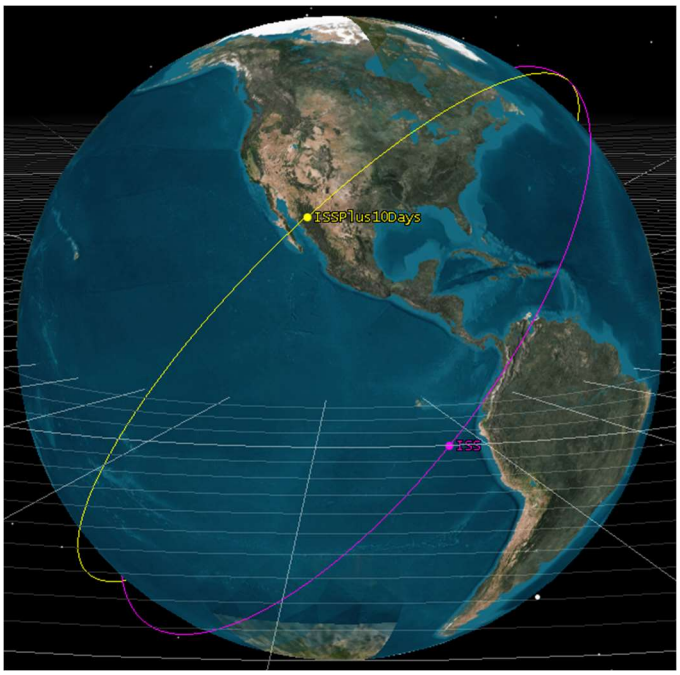

Figure 6 – ISS Nodal Precession after 100 Days

Nodal precession would therefore allow those Dream Chasers chosen to be deployed from the ISS, as well as those launched conventionally to take advantage of the Earth's shape to economically build the constellation configuration, saving ΔV and maximizing ground coverage.

Chapter 4 – Computational Methods

4.1 Computational Modeling Theory

In order to test and validate each of the configurations to be tested certain metrics will need to be evaluated in order to quantify and qualify each configuration's usefulness and practicality for disaster response for the chosen case-study area. The metrics that will be compared between each configuration after scenario simulations will be average revisit time, total coverage time, ΔV needed in each Dream Chaser to build the full constellation, and total estimated cost of deployment.

Average revisit time calculates the mean time in seconds between which a constellation asset (in STK this will be modeled by a sensor with a defined swath) can be tasked to observe a given grid-point in the ground coverage definition of the STK scenario. In practical terms, average revisit time informs the desired area how often it could, on average, be able to task a sensor on-board a Dream Chaser in the constellation configuration for EO. This metric will allow for a qualitative and quantitative comparison between configurations and currently available taskable platforms for disaster response. Average revisit time will change in time for a given area over a specified time interval, as the constellation propagates, and its assets diverge from each other predictably.

Total coverage time calculates in seconds the total time per grid-point that a constellation asset can be tasked over the course of a specified time interval. The time intervals for this metric, as for average revisit time, will be each month from July 2017 to July 2018. Total coverage time will also change in time as the constellation propagates and will give an idea of how each configuration would differ in coverage quantity in comparison to static, conventional EO platforms, which have regular tasking windows.

Average revisit time and total coverage time per latitude and longitude will be calculated in order to assess the modalities of each configuration as they propagate through each individual time interval. This progression of coverage modalities in time will be referred to as the Passive Dynamic Response of the system, as it will represent the ability of each constellation configuration to respond to certain regions for EO without maneuver inputs.

There are four total configurations that will be modelled within the scope of this paper. These configurations, for simplicity in computational modelling, will follow a Walker Delta or modified Walker Delta configuration. A Walker Delta is a satellite configuration that evenly

distributes individual nodes (satellites) at certain trajectories often to achieve better overlapping in coverage. The GPS system is an example of a Walker Delta constellation. Walker Delta notation for circular orbits is defined by the following algorithm

$$i: t/p/f \tag{10}$$

Where

i = inclination [deg]

t = number of satellites

p = number of equally spaced planes

f = relative spacing

For example, a constellation of three satellites orbiting in 3 equally spaced planes at 30° inclination could have a Walker Delta notation of **30°: 3/3/1.** The "1" denotes the phasing between neighboring planes. The separation of the true anomaly between those neighboring planes is found by **f*360/t** (Walker, 1984). Table 5 below details the basic strategies behind the 4 tested configurations.

Table 5 – Tested Walker Delta Constellation Configurations

Notation	Description	Motivation	Notes
51.64°: 5/5/1	5 DC's at 51.64° (ISS) inclination; 5 planes; equally spaced Ω and ν	Assess coverage at case-study lat/long if constellation remains at ISS inclination	-
3(51.64°); 2(30°): 5/5/1	3 DC's at 51.64° (ISS), 2 at 30° inclination; 5 planes; equally spaced Ω and ν	Split inclinations between the ISS and 30° for better coverage at lower latitudes.	Have 3 DC's deployed from ISS without need for extra ΔV, 2 with ~2,500 extra [m/s] to plane change to 30°. Nodal precession will stray constellation from Walker Delta phasing overtime.
(15°, 17.5°, 20°, 22.5°, 25°): 5/5/1	5 DC's at 15°, 17.5°, 20°, 22.5°, 25° inclinations, respectively; 5 planes; equally spaced Ω and ν	Spread focus on low to low-mid latitudes evenly; predictable but non-uniform regression of line of nodes.	Walker Delta notation only used for initialization of propagation of constellation; constellation will stray from Walker Delta phasing overtime.
15°: 5/5/1	5 DC's at 15° inclination; 5 planes; equally spaced Ω and ν	Focus on lower latitudes, predictable regression of line of nodes.	Whole system would have to be deployed conventionally, due to the enormous amount of ΔV (>4,000 [m/s]) needed to plane-change from 51.64° inc.)

Five Dream Chaser's was chosen to be the constellation number semi-arbitrarily. However, it was found upon investigation that less than four DC's in similar configurations yielded revisit times and total coverage times that were not much better than for traditional systems, with much less global coverage. The altitude of each Dream Chaser was chosen to be 701 kilometer, allowing the constellation to be propagated within a practical real-world time frame of about 120 days.

4.2 Systems Tool Kit® Scenario Set-up

In order to run test each constellation for metric, the scenarios must be initiated in STK, with constraints set in place in order to limit computational power and time needed. The first step was to define the scenario interval, which would be the minimum and maximum bounds for propagation for every asset in the scenario. This was set from the aforementioned datum of **05 Jul 2017 06:28:58 UTC** to **05 Aug 2018 06:28:58 UTC** in order to analyze a full-year period for each constellation.

The next step was to define the ground coverage area to be evaluated for coverage metrics. Shapefiles for the major countries within the ASEAN region and Indian subcontinent were uploaded from the STK Standard Object Database (SOD) and overlaid over the 2D projection within the workspace. The resolution was set at ±1° latitude and longitude in order to precisely map smaller areas such islands in the Philippines, Indonesia, and Malaysia. Figure 7 on the following page displays the ground coverage definition from STK.

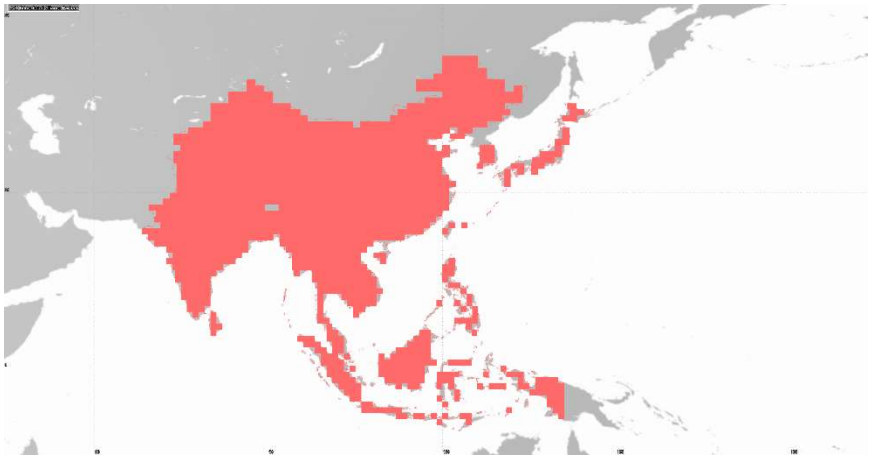

Figure 7 – STK Area Definition for EO Ground Coverage Analysis

Given the chosen epoch of 05 Jul 2017 06:28:58 UTC, the ISS Zarya (25544) module was initialized in an STK scenario workspace in order to be the reference of ephemerides for the Dream Chasers to be propagated forward. The ISS is propagated with the Simplified General Perturbations (SGP4) propagator, which pulls Two-Line Elements (TLEs) from the NASA database at regular intervals to correct for complex perturbations such as orbital drag or Lunar-Solar perturbations.

To ensure that the ground coverage definition area only computes sensor accesses in direct daylight (eliminating data points during which sensors are above the area under the penumbra of the Earth), a default facility object with the direct sunlight constraint was inserted into the scenario. The constraint was then associated to the entire coverage area.

Then, for each constellation configuration, the five Dream Chasers were inserted into the scenario as default satellites with negligible ballistic profiles. The propagator for each was set as the J_2 Propagator, in order to simply analyze the progression of each trajectory with the only force input the oblation of Earth and therefore nodal precession. Figure 8 on the following page is an example of one of the satellite objects, this one being the initial Dream Chaser of the 51.64°: 5/5/1 configuration.

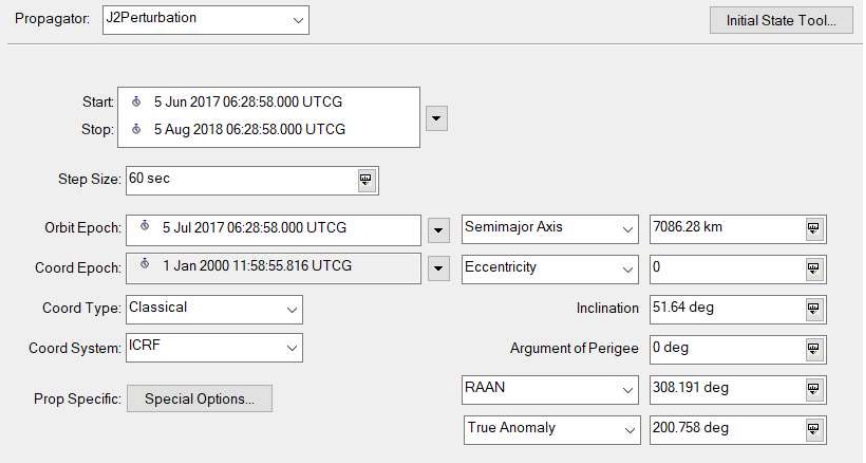

Figure 8 – Example of Dream Chaser Satellite Object Initialization

This was done for every Dream Chaser in each configuration, and the true anomaly and RAAN were varied according to the Walker Delta separation algorithm. The step size of 60 seconds was chosen by default by STK.

Sensor models were then attached to each Dream Chaser. These would be associated to the grid-points in the ground coverage definition when a constellation asset is overhead, thereby starting the clock for both the revisit time and total coverage time figures of merit. These sensors were modelled as simple rectangular push-broom sensors, with a cross-track half angle of 15°, and an along-track half angle of 5°. This was chosen in order to represent a generic SAR or similar multispectral sensor.

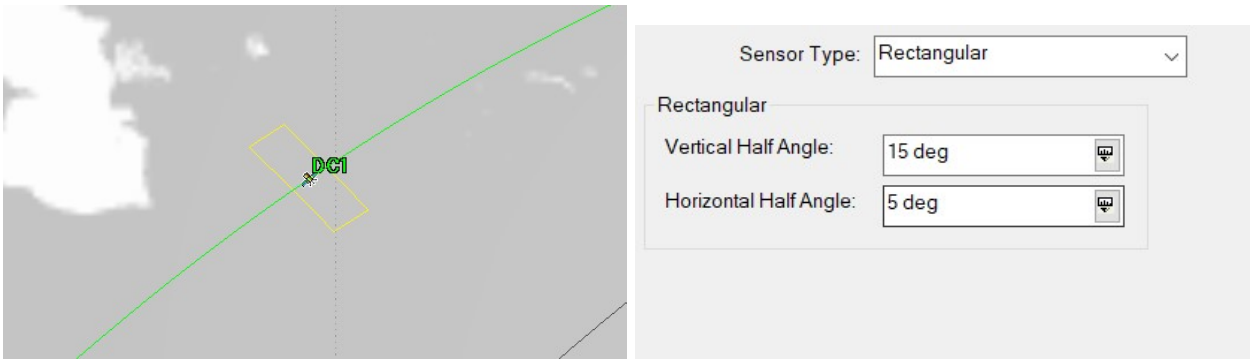

Figure 9 – Sensor Object Definition for each Dream Chaser

The Dream Chaser constellation could then be applied to the ground coverage definition as active assets, determining what sensors the grid-points were looking for as accesses as the

scenario interval went through in time.

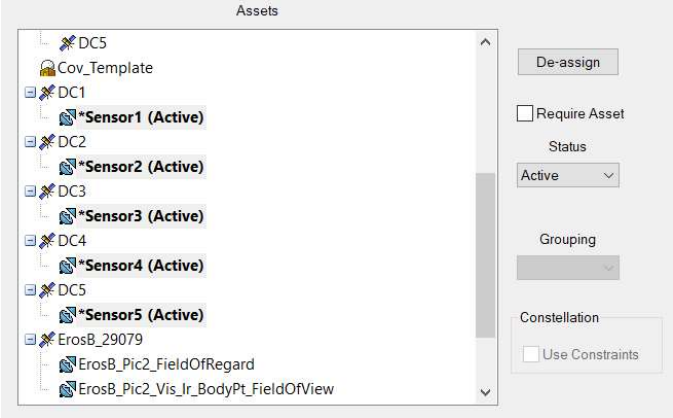

Figure 10 – Ground Coverage Definition Assets

4.3 Data Output

With the scenarios set up completely in STK, the average revisit time and total coverage time figures of merit had to be inserted into the scenario workspace. A figure of merit outputs the appropriate data from the ground coverage definition over the simulation, in this case average revisit time and total coverage time per each month of each configuration from July 2017 to July 2018. The graphical output for each month and each figure of merit would be screenshotted and plotted against the other months, utilizing a heat-map graphical approach. Figure 11 below contains an example for average revisit time for a configuration interval.

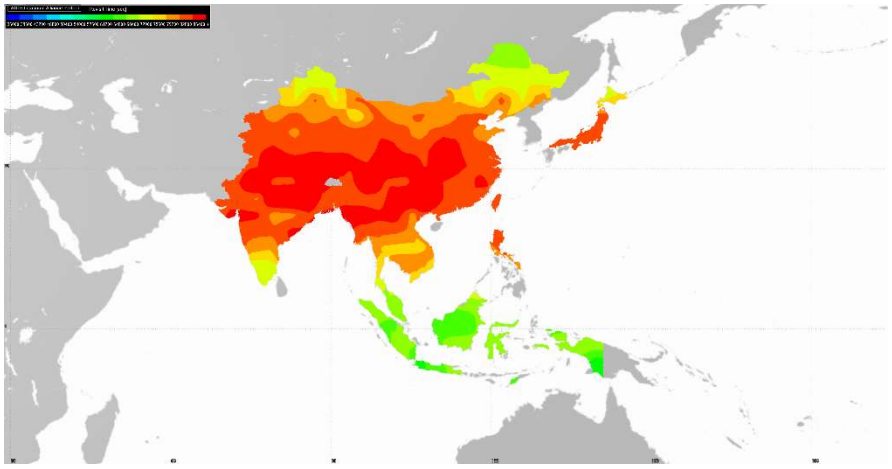

Figure 11 – Example Graphical Output in STK for Figure of Merit

The color contours for each scenario would be chosen subjectively according to average time scales, each within a minimum and maximum number of seconds.

Chapter 5 – Results and Analysis

Figure 12 on page 27 displays visuals from STK that chart the average revisit time in seconds over each interval for the Walker Delta configuration of three Dream Chasers at the ISS inclination of 51.64°, and two at an inclination of 30°, all at an altitude of 700 kilometers (3(51.64°); 2(30°):/5/5/1). It can be seen that there is a certain period by which the configuration rotates throughout its nodal plane, thereby repeating revisit time modalities for certain latitudes and longitudes. This example and the proceeding examples showcase the Passive Dynamic Response (in which no ΔV is imparted once satellite constellation configuration is completed) of such a system, whereby the epoch of the configuration can be adjusted so that favorable coverage aligns with extreme weather seasons in areas highly susceptible to extreme weather patterns such as Vietnam or the Philippines.

This specific configuration saves the maximum amount of ΔV for the three Dream Chasers deployed from the ISS by only undergoing an altitude change, allowing for future work to analyze possibilities of active response to random events on the globe by the Active Dynamic Response capabilities of the configuration. The two Dream Chasers at 30° inclination would either have to be deployed conventionally through launch from a launch pad such as the ones at Cape Canaveral, or else the Dream Chasers would have to be heavily modified with tons of propellant.

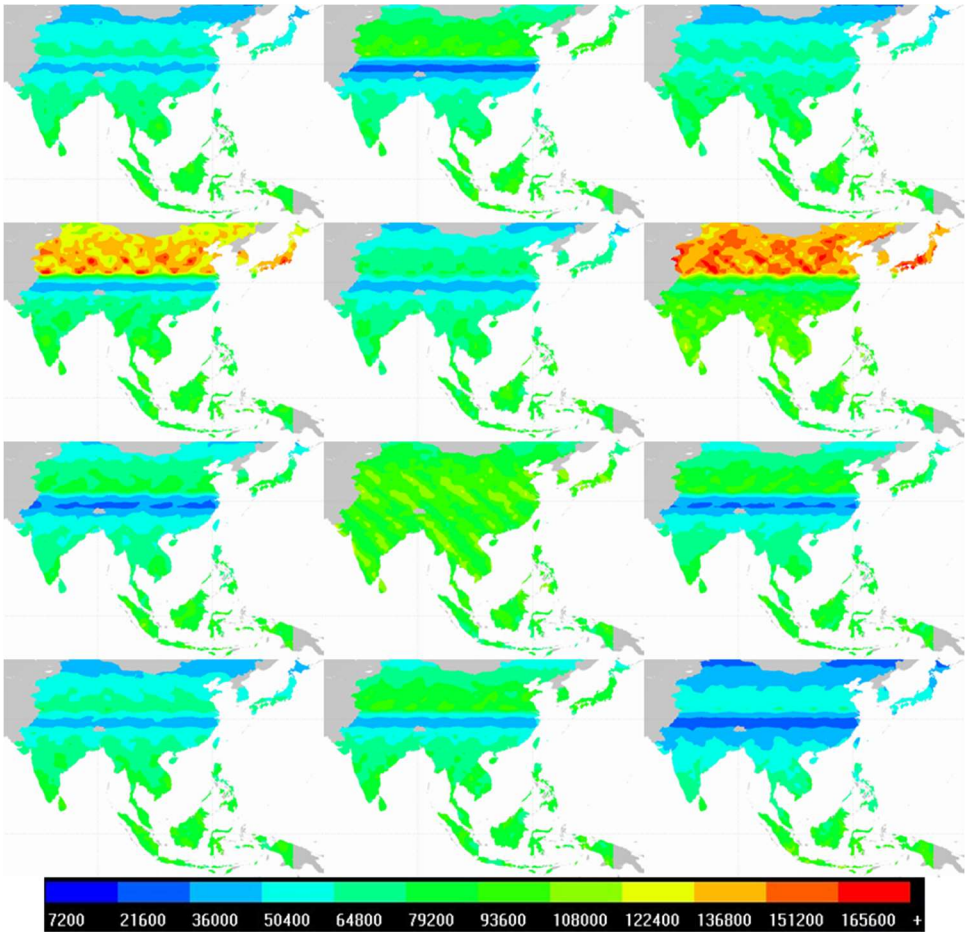

Figure 12 – 3(51.64°); 2(30°):/5/5/1 Average Revisit Times in **Seconds** Read left to right, top to bottom. [top left: Jul-Aug 2017, bottom right: Jun-Jul 2018]

Similarly, Figure 13 on the following page displays the total coverage time for the same configuration and shows similar passive modality characteristics. Again, this configuration focuses more heavily on certain latitudes and longitudes during specific times of the interval, again showing the Passive Dynamic Response characteristics that this approach to remote-sensing could provide.

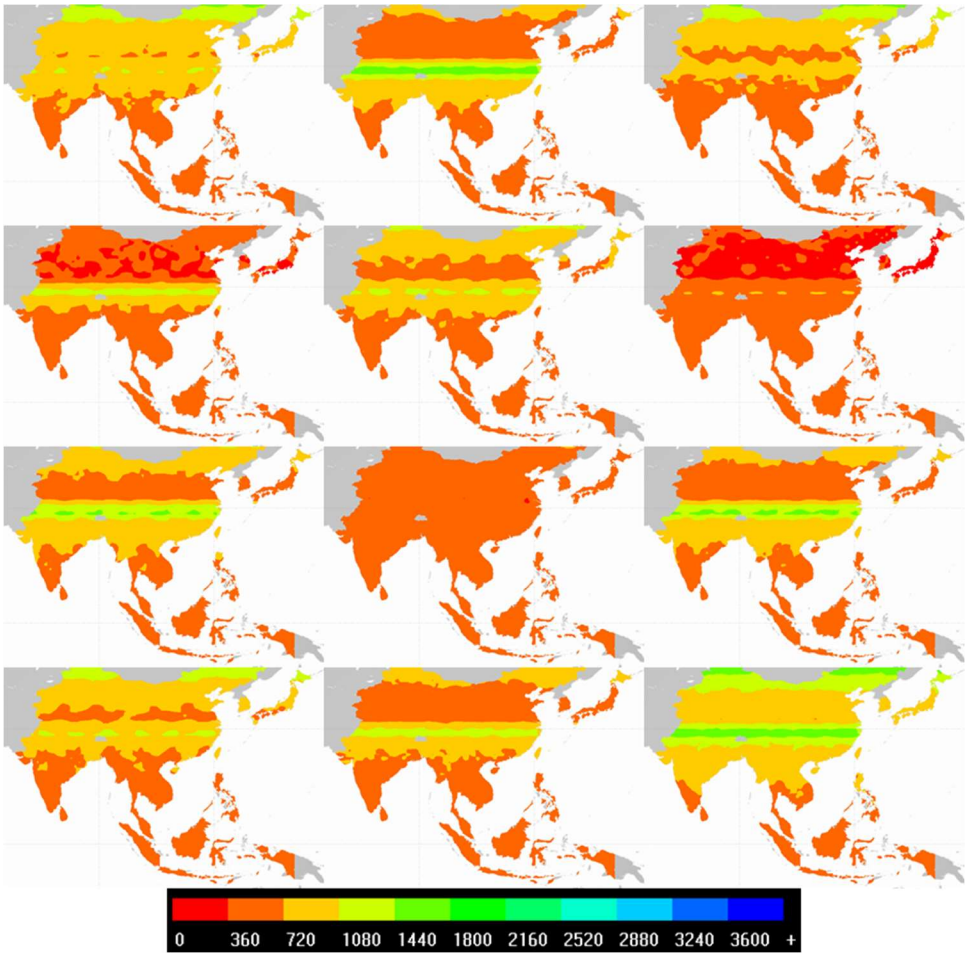

Figure 13 – 3(51.64°); 2(30°):/5/5/1 Total Coverage Times in **Seconds** Read left to right, top to bottom. [top left: Jul-Aug 2017, bottom right: Jun-Jul 2018]

The same graphics for the three other configurations can be found in Appendix A, along with graphs for the average revisit and total coverage times for the full year scenario. They all displayed the same sort of tunable response modalities for coverage, each with different pros and cons. For the two configurations that utilized the ISS inclination, it was found that although the lower latitudes, such as where Indonesia and Malaysia sit, revisit times were much lower than up near the ISS inclination. These average revisit times were still on average less than conventional systems, with times on the magnitudes of days and a half instead of a few days. This configuration also provided sort of a template for the other configurations, as it was the least modified. For future work, this configuration could be the model on which the Active Dynamic Response properties of

the system could be tested, wherein the Dream Chasers respond in real time to a random event on the ground via active burning of propellant. The configuration with the two Dream Chasers placed at 30° inclination while the other three were at ISS showed better average revisit times and total coverage times for those lower latitudes, as was expected. However, the two 30° inclined Dream Chasers would have to be launched conventionally, thereby greatly increasing the cost of such a configuration. The two lowly inclined configurations showed greatly reduced revisit times, on the order of every few hours for latitudes that lined up with Dream Chaser inclinations, with total coverage time each month also on the order of hours. However, these two would be the most expensive implementation of such a system by far, as they would not be able to utilize ISS deployment following CRS-2 missions at all, as the ΔV for those plane change maneuvers from 51.64° would force the Dream Chasers to carry tens of thousands of extra kilograms of propellant. So, they would have to be launched conventionally. However, these are by far the best options for response to ground events if money is no object.

All configurations regardless of their pros and cons display Passive Dynamic Response capabilities such a system could provide, whereby the epoch and configuration of the constellation could be the factor that decides which times of the year certain key locations on the ground can receive ground coverage that allows them to get near-real time data for disaster response purposes.

Chapter 6 – Conclusion

We have introduced the idea for a dynamic, maneuverable constellation of Sierra Nevada Dream Chasers and presented initial orbital calculations and configurations and assessed their modalities for ground coverage. What can be shown is that while a non-traditional constellation not in a polar orbit limits the total coverage area on the ground, that constellation with proper maneuverable capabilities can be adjusted in its epoch and configuration to target key areas on the globe at key times for more frequent tasking. More frequent tasking would prove an asset to any country, especially those in the ASEAN region, looking to respond economically and effectively to climate disasters, allowing responders on the ground more data on how to react.

Such a system would be maximized in its economic feasibility if used as a "piggy backing" mission after each Dream Chaser's completion of its CRS-2 mission to the ISS with NASA. In avoiding launch, research and development of conventional satellite components, and testing and validation costs, such a system operated by a third party to SNC or NASA could save billions of dollars in its creation, deployment, and operation. This economic approach would however then be most noticeable by disaster relief actors in regions identified as targets for EO from this system, who would likely be able to task this highly dynamic, potentially modular system cheaper, more rapidly, and more reliably than conventional EO platforms.

This system would also allow for upgrades to the individual Dream Chasers' with new and improved instrumentation as each Dream Chaser completes its mission interval, deorbits, and is refitted with different and better instruments. The reusability of the vehicles would therefore allow for modularity, something that is not possible with conventional EO platforms.

This potential system would satisfy all of the gaps in the current space community discussed in the background information of this paper, allowing for shorter revisit times and more

robust remote-sensing for disaster response for areas of the globe and peoples that need it most. Its economic sustainability and feasibility fits perfectly within the current culture of the New Space movement, whereby space is brought down to the colloquial level and is made available to all.

Appendix A – Coverage Modalities

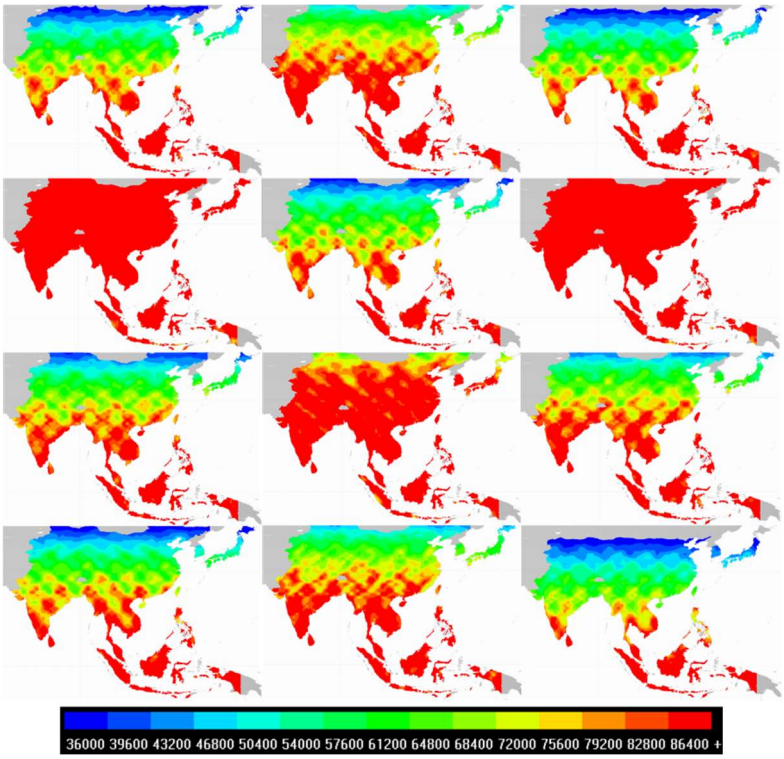

Figure A1 – 51.64°:/5/5/1 Average Revisit Times in **Seconds** Read left to right, top to bottom. [top left: Jul-Aug 2017, bottom right: Jun-Jul 2018]

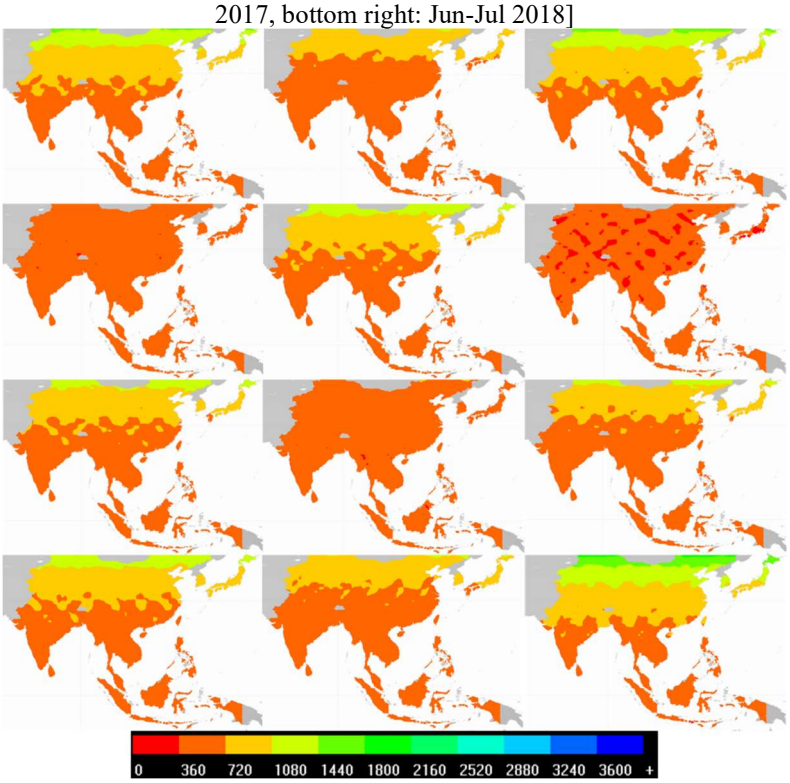

Figure A2 – 51.64°:/5/5/1 Total Coverage Times in **Seconds** Read left to right, top to bottom. [top left: Jul-Aug 2017, bottom right: Jun-Jul 2018]

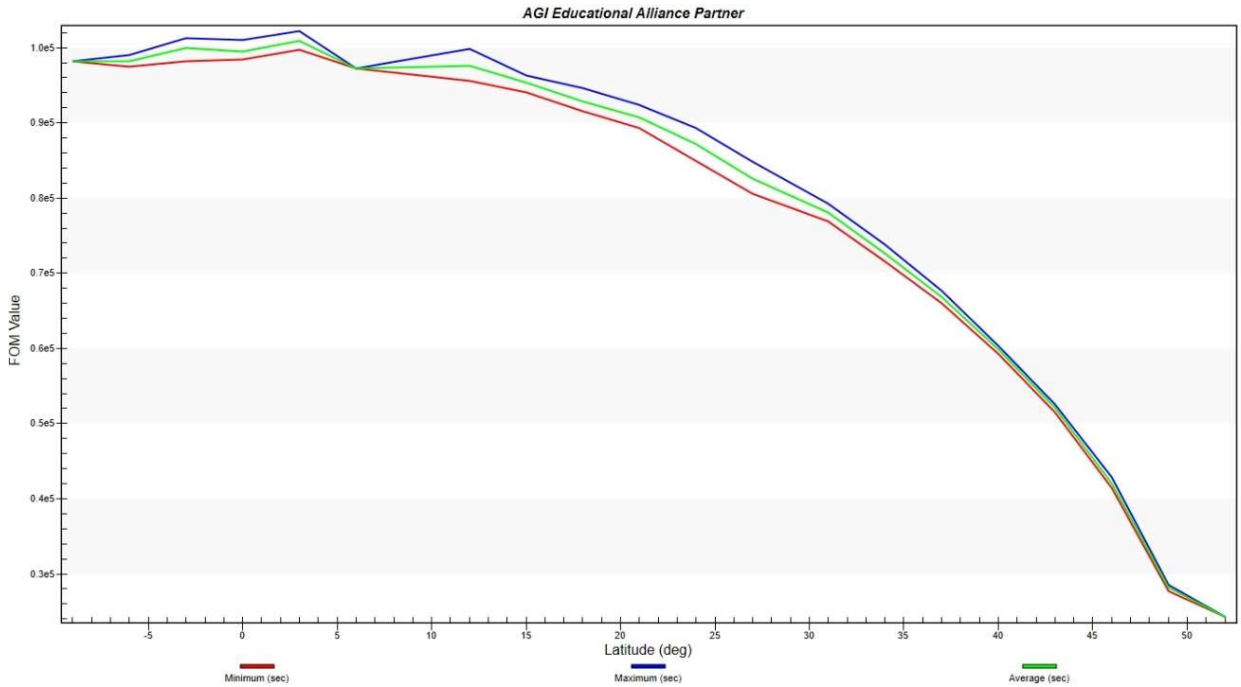

Figure A3 – 51.64°:/5/5/1 Average Revisit Time Per Latitude over Full Scenario Interval
[y-axis in **seconds**]

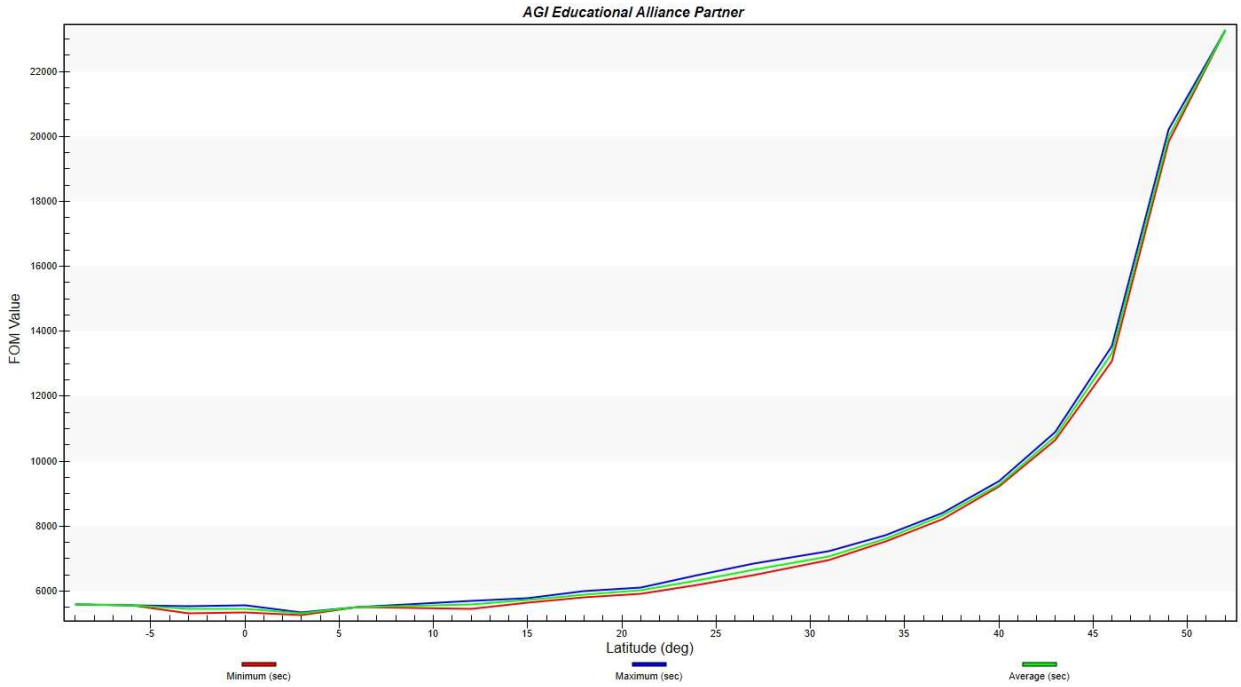

Figure A4 – 51.64°:/5/5/1 Coverage Time Per Latitude over Full Scenario Interval
[y-axis in **seconds**]

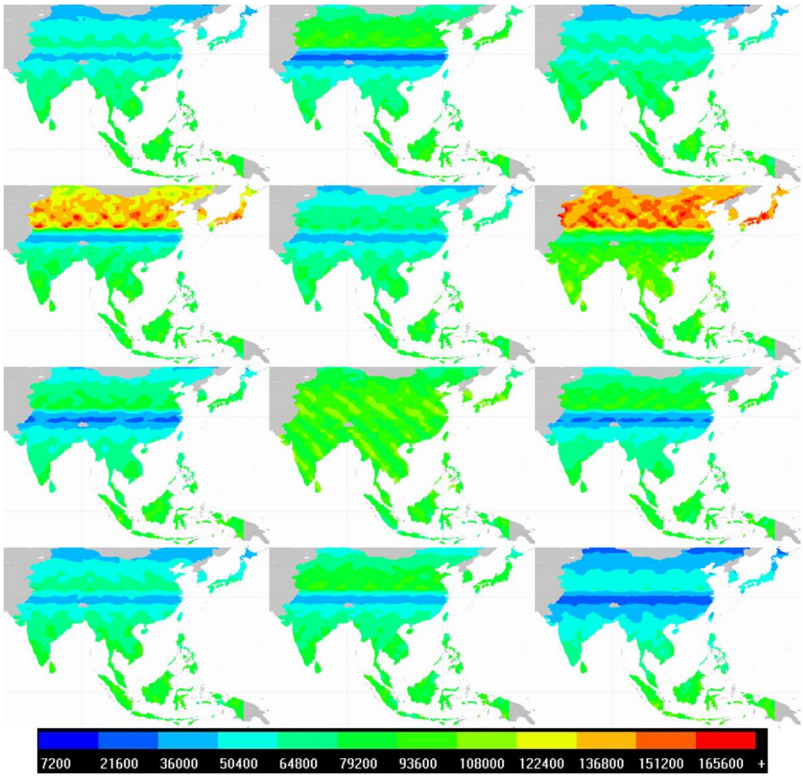

Figure A5 – 3(51.64°); 2(30°):/5/5/1 Average Revisit Times in **Seconds** Read left to right, top to bottom. [top left: Jul-Aug 2017, bottom right: Jun-Jul 2018]

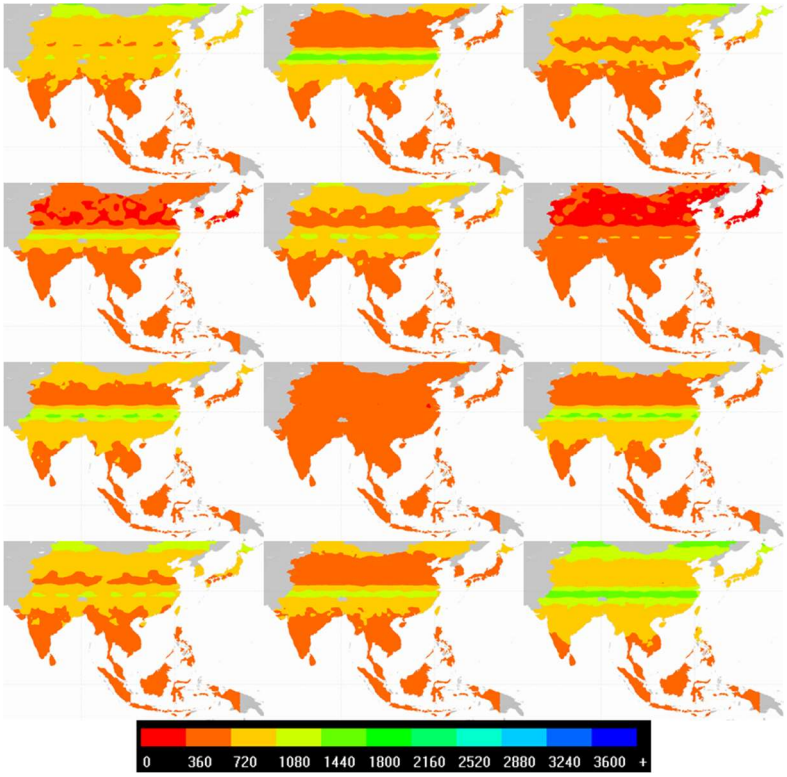

Figure A6 – 3(51.64°); 2(30°):/5/5/1 Total Coverage Times in **Seconds** Read left to right, top to bottom. [top left: Jul-Aug 2017, bottom right: Jun-Jul 2018]

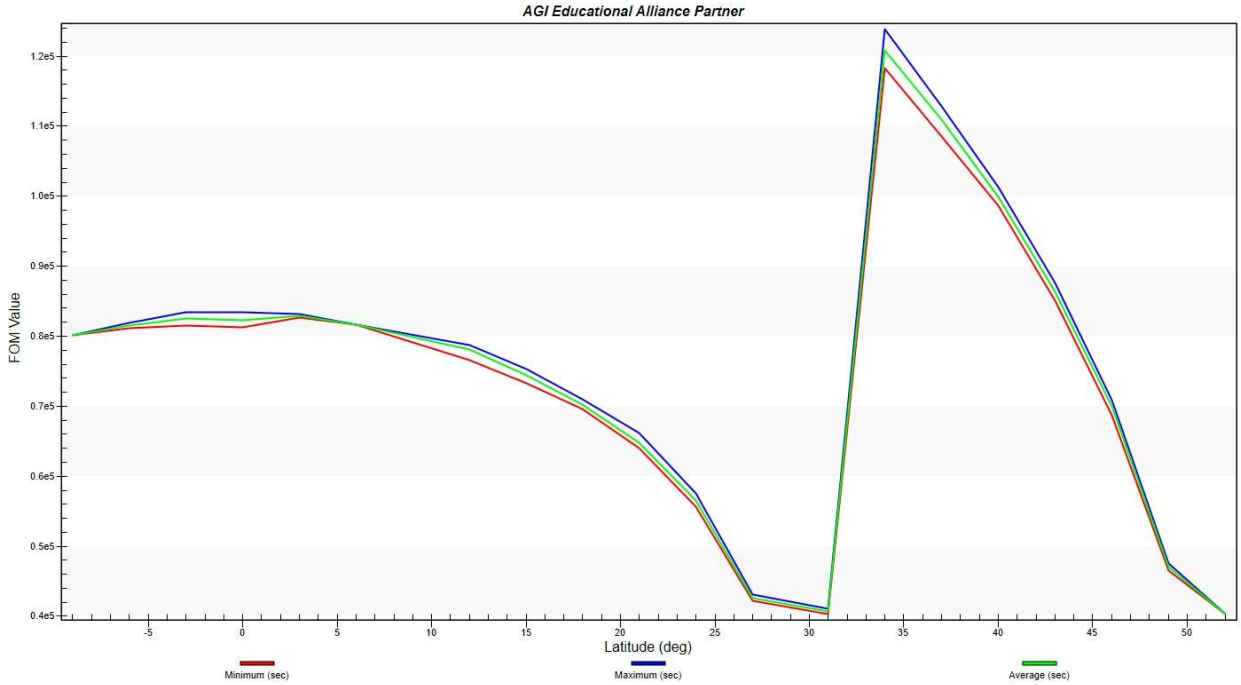

Figure A7 – 3(51.64°); 2(30°):/5/5/1 Average Revisit Time Per Latitude over Full Scenario Interval [y-axis in **seconds**]

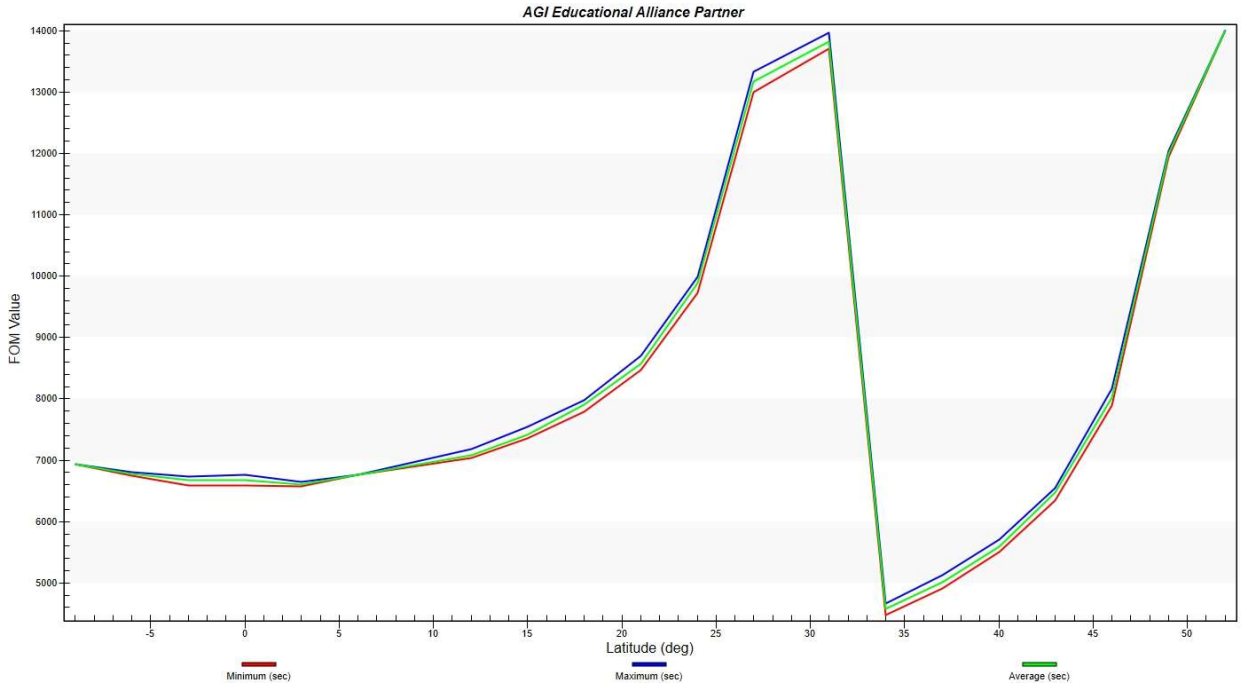

Figure A8 – 3(51.64°); 2(30°):/5/5/1 Coverage Time Per Latitude over Full Scenario Interval [y-axis in **seconds**]

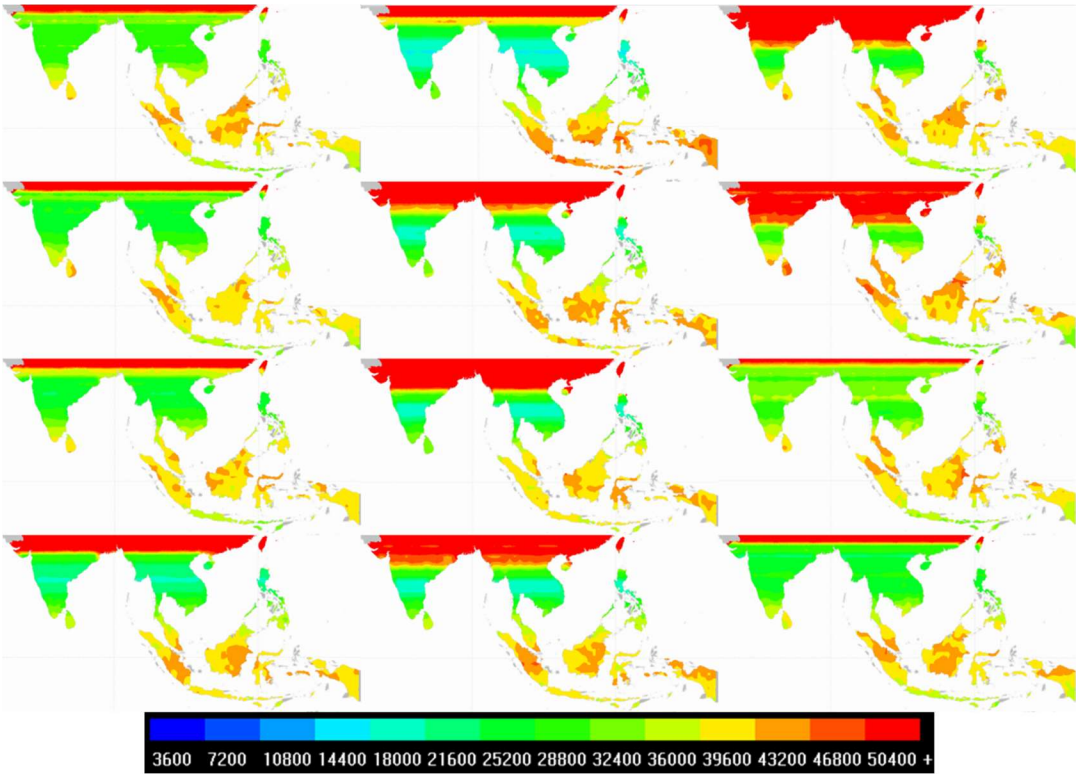

Figure A9 – (15°, 17.5°, 20°, 22.5°, 25°): 5/5/1 Average Revisit Times in **Seconds** Read left to right, top to bottom. [top left: Jul-Aug 2017, bottom right: Jun-Jul 2018]

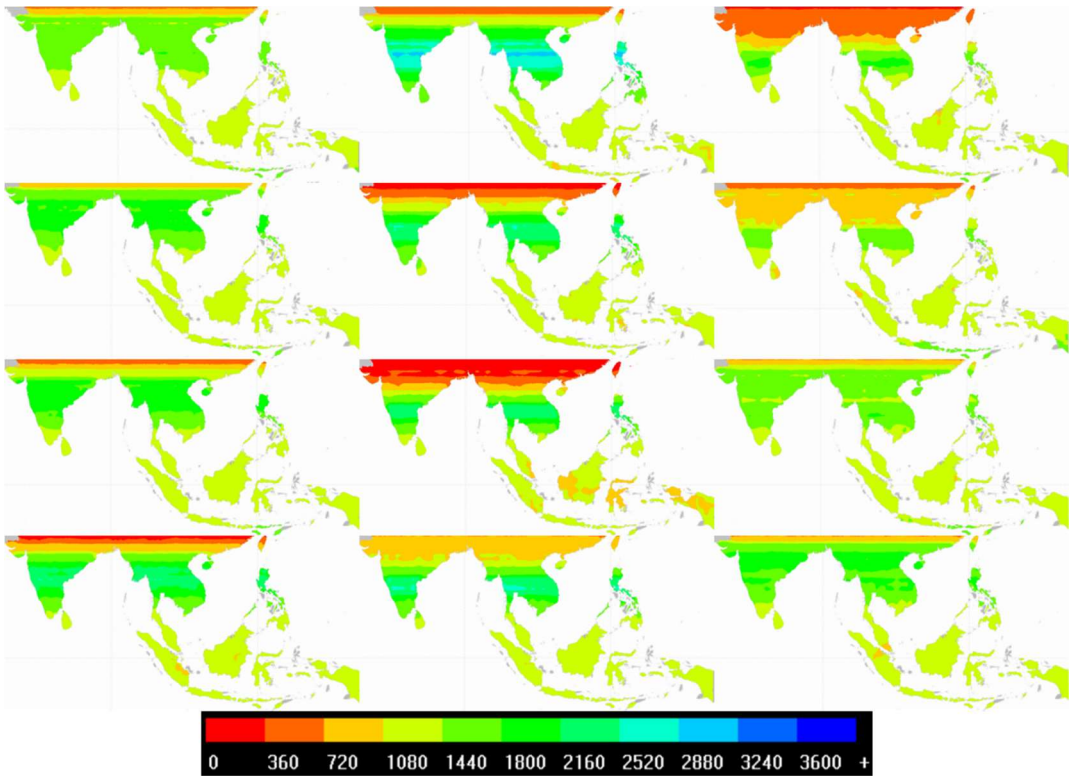

Figure A10 – (15°, 17.5°, 20°, 22.5°, 25°): 5/5/1 Total Coverage Times in **Seconds** Read left to right, top to bottom. [top left: Jul-Aug 2017, bottom right: Jun-Jul 2018]

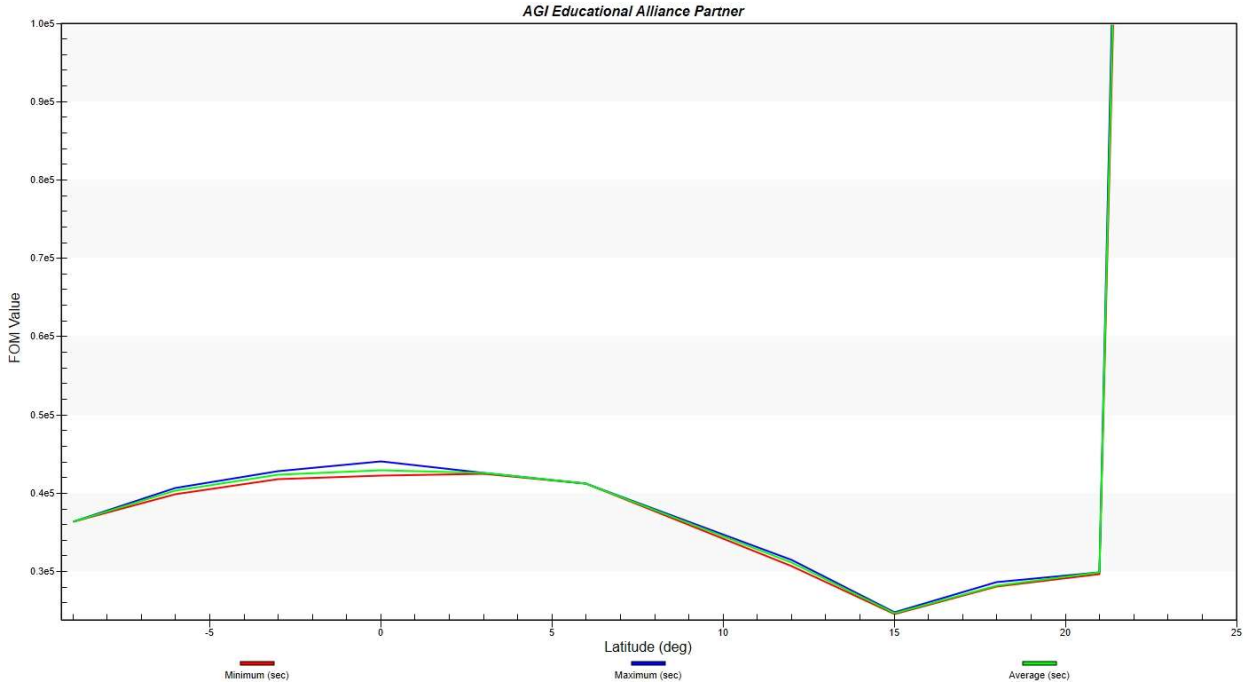

Figure A11 – (15°, 17.5°, 20°, 22.5°, 25°): 5/5/1 Average Revisit Time Per Latitude over Full Scenario Interval [y-axis in **seconds**]

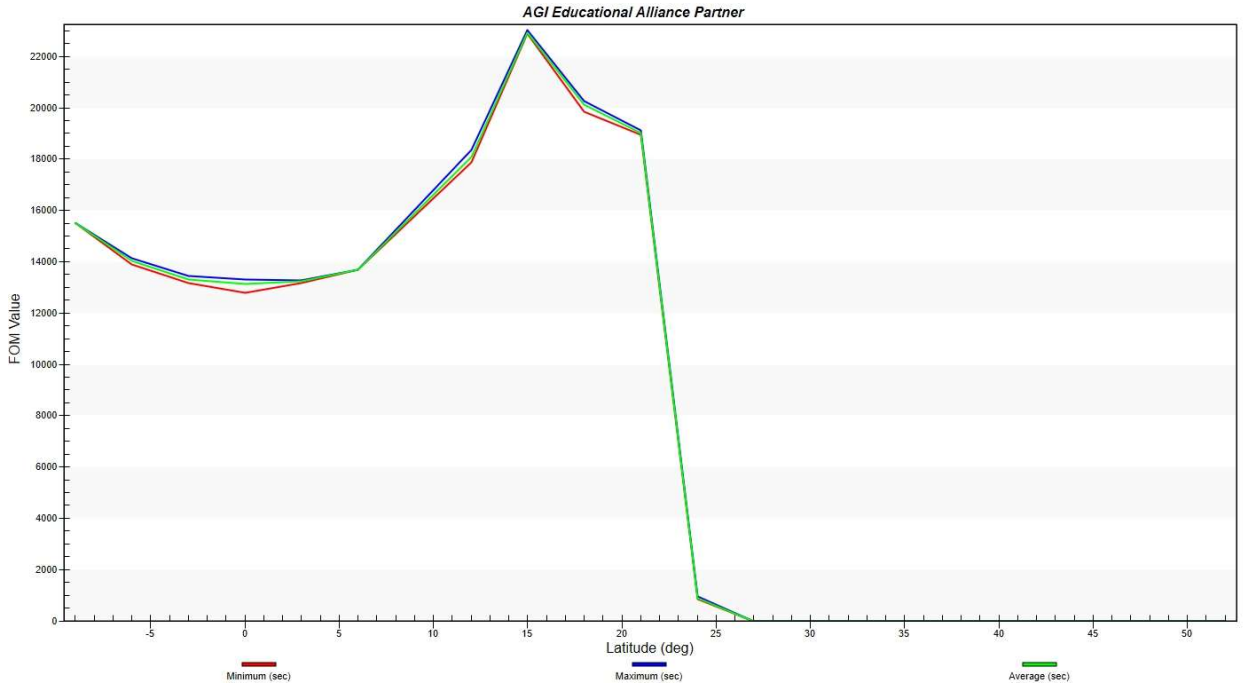

Figure A12 – (15°, 17.5°, 20°, 22.5°, 25°): 5/5/1 Coverage Time Per Latitude over Full Scenario Interval [y-axis in **seconds**]

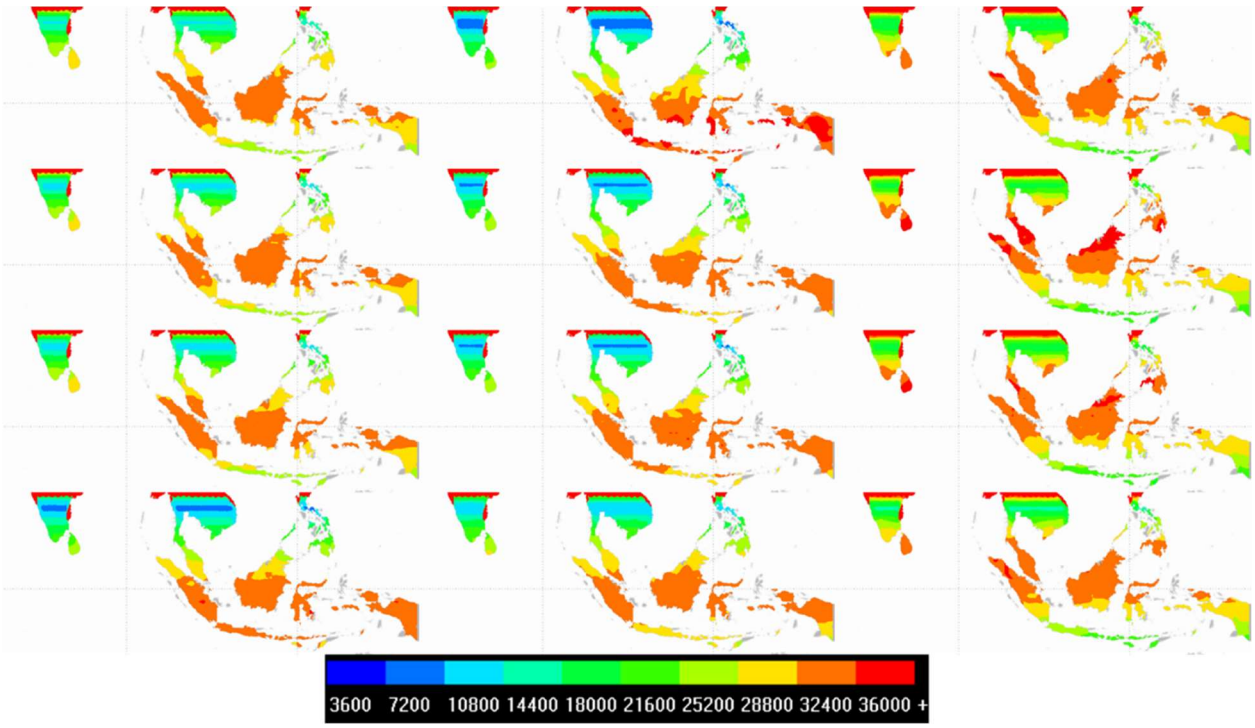

Figure A13 – 15°: 5/5/1 Average Revisit Times in **Seconds** Read left to right, top to bottom. [top left: Jul-Aug 2017, bottom right: Jun-Jul 2018]

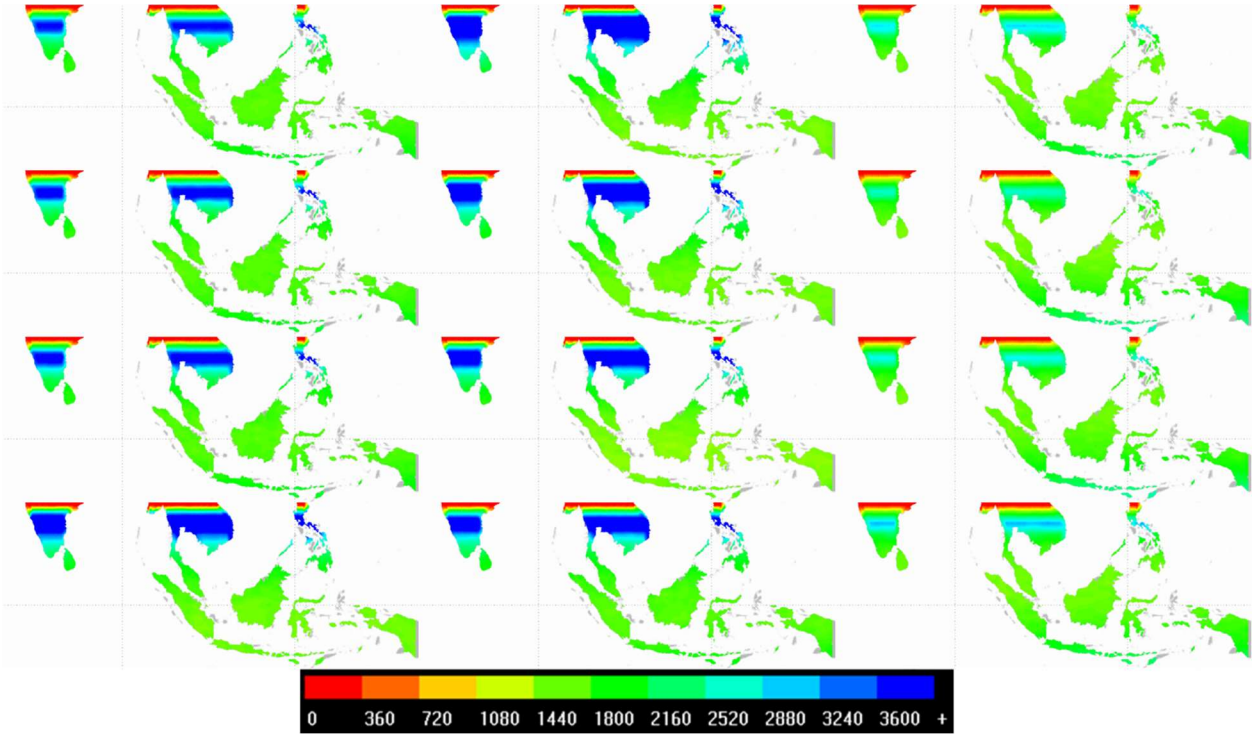

Figure A14 – 15°: 5/5/1 Total Coverage Times in **Seconds** Read left to right, top to bottom. [top left: Jul-Aug 2017, bottom right: Jun-Jul 2018]

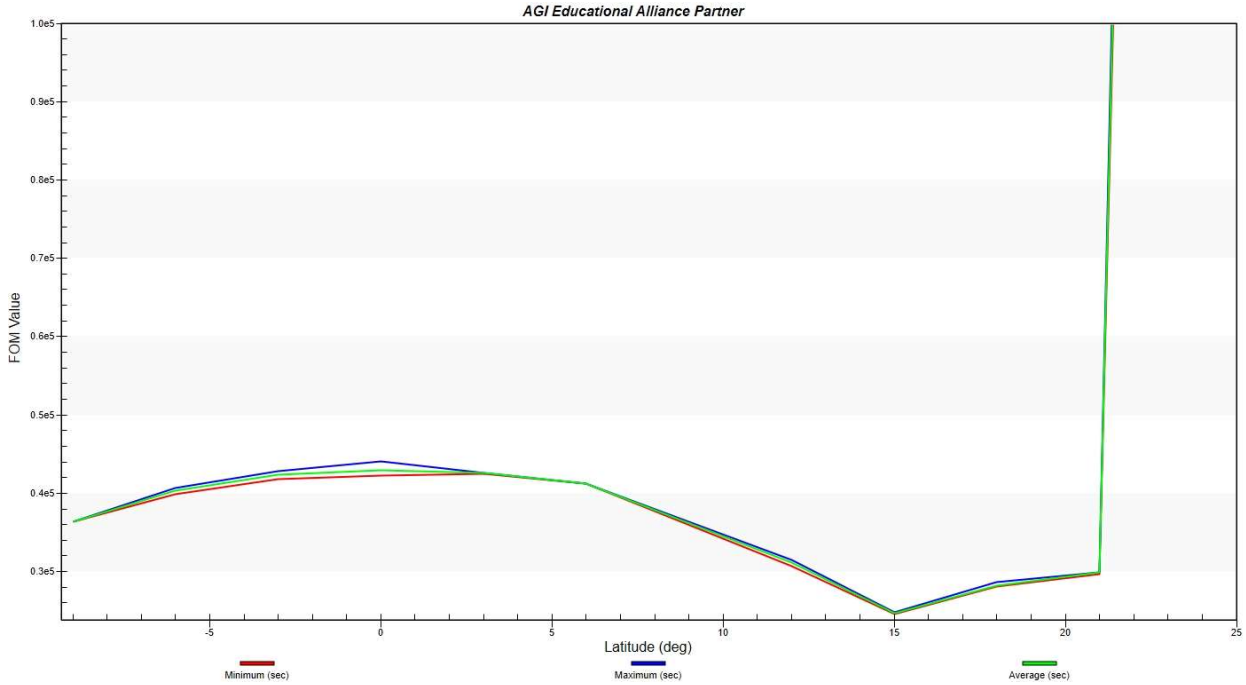

Figure A15 – 15°: 5/5/1 Average Revisit Time Per Latitude over Full Scenario Interval
[y-axis in **seconds**]

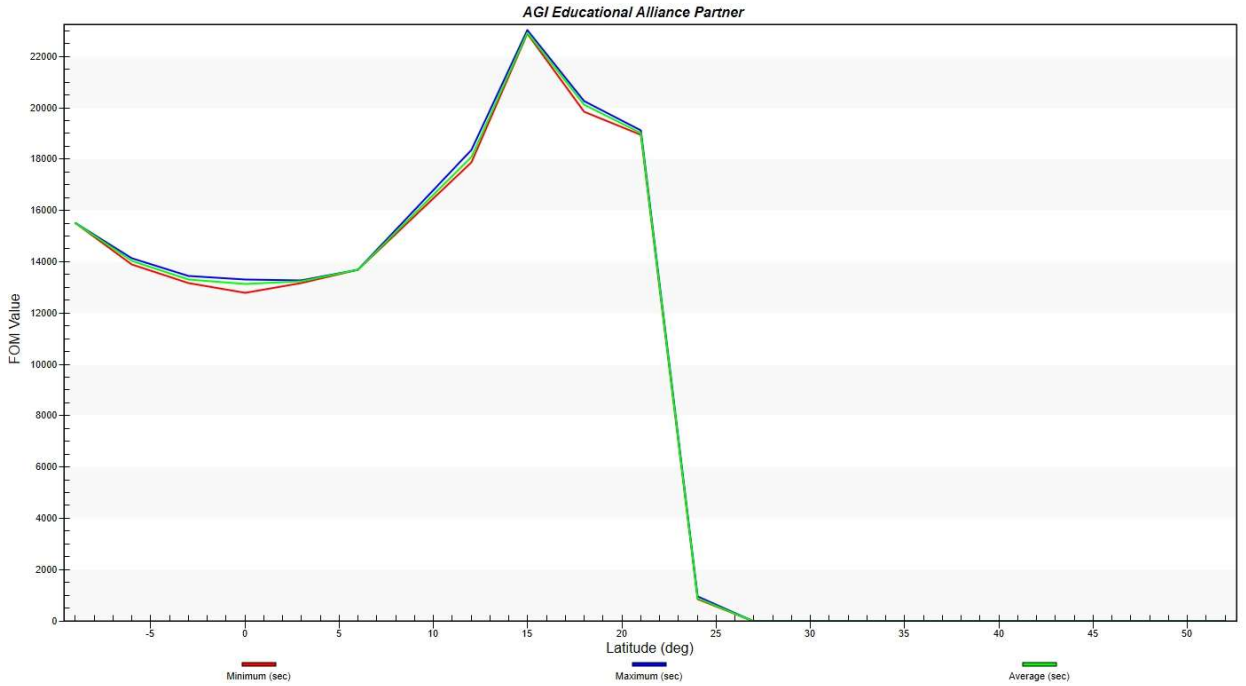

Figure A16 – 15°: 5/5/1 Coverage Time Per Latitude over Full Scenario Interval
[y-axis in **seconds**]

Appendix B

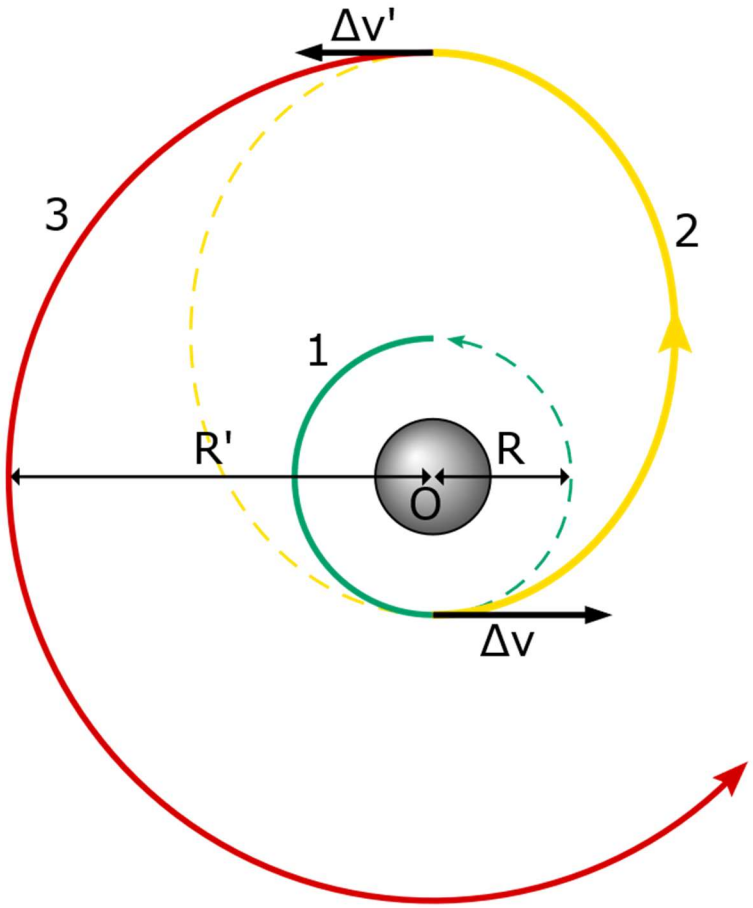

Figure B1 – Example of Typical Hohmann Transfer Strategy

References

Chaikin, Andrew. (2012). Is SpaceX Changing the Rocket Equation. *AirSpaceMag.com*. Air & Space Smithsonian. Retrieved from https://www.airspacemag.com/space/is-spacex-changing-the-rocket-equation-132285884/?no-ist

Cheng, L., K. E. Trenberth, J. Fasullo, J. Abraham, T. P. Boyer, K. von Schuckmann, and J. Zhu (2017), Taking the pulse of the planet, *Eos, 98,* doi:10.1029/2017EO081839. Published on 13 September 2017.

Cruz, R.V., H. Harasawa, M. Lal, S. Wu, Y. Anokhin, B. Punsalmaa, Y. Honda, M. Jafari, C. Li and N. Huu Ninh, 2007: Asia. *Climate Change 2007: Impacts, Adaptation and Vulnerability. Contribution of Working Group II to the Fourth Assessment Report of the Intergovernmental Panel on Climate Change*, M.L. Parry, O.F. Canziani, J.P. Palutikof, P.J. van der Linden and C.E. Hanson, Eds., Cambridge University Press, Cambridge, UK, 469-506.

Griffin, Michael D., French, James R. (2004). Astrodynamics. In *Space Vehicle Design, Second Edition* (pp. 140-142). Reston, VA: AIAA

Knutson, Thomas R., et al. (2010), Tropical cyclones and climate change, *Nature Geoscience, 3,* doi:10.1038/ngeo779. Published on 21 February 2010.

List of cities by population density. (2018), Wikipedia. Retrieved from https://en.wikipedia.org/wiki/List_of_cities_by_population_density

Olson, John, (2014), Getting There and Back: Dream Chaser [.ppt], *astronautical.org*. Sierra Nevada Corporation. Retrieved from www.astronautical.org/sites/default/files/attachment/AAS%20ISS%20R%26D%20Brief%20Jun%202014%20vGO.pdf

Selected basic ASEAN indicators [.pdf]. (2014), *ASEAN.org*. ASEANstats. Retrieved from https://web.archive.org/web/20150904103519/http://www.asean.org/images/2015/January/selected_key_indicators/Summary%20table_as%20of%20December%202014_R.pdf

South Asia: Flooding – Humanitarian Snapshot [.pdf]. (2017), United Nations Office for the Coordination of Humanitarian Affairs. Published on 24 August 2017. Retrieved from https://reliefweb.int/sites/reliefweb.int/files/resources/SouthAsia_240817.pdf

Sutton, George P., Biblarz, Oscar. (2010). Hybrid Propellant Rockets. In *Rocket Propulsion Elements, Eighth Edition* (pp. 594-621). Hoboken, NJ: John Wiley & Sons, Inc.

Viet Nam: Typhoon Damrey & Flooding in the Central and Highland Regions of Viet Nam, Situation Update No. 4 (as of 13 December 2017). (n.d.). Retrieved March 28, 2018, from https://reliefweb.int/report/viet-nam/viet-nam-typhoon-damrey-flooding-central-and-highland-regions-viet-nam-situation-0

Walker, J.G., (1984). Satellite constellation, *Journal of the British Interplanetary Society, 37 (*pp. 559-571)

Walter, L.S. (1990), The uses of satellite technology in disaster management. *Disasters, 14(1)*, doi: 10.1111/j.1467-7717.1990.tb00969.x. Published in March 1990.

World Bank Open Bank. (2018), The World Bank Group. Retrieved from https://data.worldbank.org/